

**Award Number:** W81XWH-09-1-0314

**TITLE:** Molecular targeting of prostate cancer during androgen ablation: inhibition of  
CHES1/FOXN3

**PRINCIPAL INVESTIGATOR:** Clifford G. Tepper, Ph.D.

**CONTRACTING ORGANIZATION:** University of California  
Davis, CA 95618-6134

**REPORT DATE:** May 2012

**TYPE OF REPORT:** Annual

**PREPARED FOR:** U.S. Army Medical Research and Materiel Command  
Fort Detrick, Maryland 21702-5012

**DISTRIBUTION STATEMENT:** Approved for Public Release;  
Distribution Unlimited

The views, opinions and/or findings contained in this report are those of the author(s) and should not be construed as an official Department of the Army position, policy or decision unless so designated by other documentation.

<b>REPORT DOCUMENTATION PAGE</b>			<i>Form Approved</i> <i>OMB No. 0704-0188</i>		
Public reporting burden for this collection of information is estimated to average 1 hour per response, including the time for reviewing instructions, searching existing data sources, gathering and maintaining the data needed, and completing and reviewing this collection of information. Send comments regarding this burden estimate or any other aspect of this collection of information, including suggestions for reducing this burden to Department of Defense, Washington Headquarters Services, Directorate for Information Operations and Reports (0704-0188), 1215 Jefferson Davis Highway, Suite 1204, Arlington, VA 22202-4302. Respondents should be aware that notwithstanding any other provision of law, no person shall be subject to any penalty for failing to comply with a collection of information if it does not display a currently valid OMB control number. <b>PLEASE DO NOT RETURN YOUR FORM TO THE ABOVE ADDRESS.</b>					
<b>1. REPORT DATE</b> May 2012		<b>2. REPORT TYPE</b> Annual		<b>3. DATES COVERED</b> 15 April 2011 – 14 April 2012	
<b>4. TITLE AND SUBTITLE</b>  Molecular targeting of prostate cancer during androgen ablation: Inhibition of CHES1/FOXN3			<b>5a. CONTRACT NUMBER</b>		
			<b>5b. GRANT NUMBER</b> W81XWH-09-01-0314		
			<b>5c. PROGRAM ELEMENT NUMBER</b>		
<b>6. AUTHOR(S)</b>  Clifford G. Tepper, Nong Xiang, Shawn M. Purnell  E-Mail: cgtepper@ucdavis.edu			<b>5d. PROJECT NUMBER</b>		
			<b>5e. TASK NUMBER</b>		
			<b>5f. WORK UNIT NUMBER</b>		
<b>7. PERFORMING ORGANIZATION NAME(S) AND ADDRESS(ES)</b>  University of California, Davis 1850 Research Dr., Ste. 300 Davis, CA 95618-6134			<b>8. PERFORMING ORGANIZATION REPORT NUMBER</b>		
<b>9. SPONSORING / MONITORING AGENCY NAME(S) AND ADDRESS(ES)</b> U.S. Army Medical Research and Materiel Command Fort Detrick, Maryland 21702-5012			<b>10. SPONSOR/MONITOR'S ACRONYM(S)</b>		
			<b>11. SPONSOR/MONITOR'S REPORT NUMBER(S)</b>		
<b>12. DISTRIBUTION / AVAILABILITY STATEMENT</b> Approved for Public Release; Distribution Unlimited					
<b>13. SUPPLEMENTARY NOTES</b>					
<b>14. ABSTRACT</b> Our operating hypothesis is that <i>Checkpoint suppressor 1 (CHES1)/FOXN3</i> is an androgen withdrawal-induced gene that promotes prostate cancer (PCa) resistance to apoptosis. The purposes of this research are two-fold. The first is to define the mechanisms of <i>CHES1</i> gene expression regulation and function, particularly in mediating apoptosis resistance during androgen ablation. Secondly, the tools yielded from our functional studies will be utilized to test the efficacy of <i>CHES1</i> -silencing therapy (CST) in preventing castration-resistant prostate cancer (CRPC) and to develop a mechanism-based noninvasive imaging strategy for monitoring the success of CST. Several significant findings were made. We defined the mechanisms through which <i>CHES1</i> coordinates anti-apoptotic pathways, specifically enhanced PI3K/Akt activation and global regulation of genes negatively regulating apoptosis. We elucidated that <i>CHES1</i> -mediated AR repression diminishes amino acid-activated mTORC1, which consequently de-represses PI3K-Akt activity. We defined the precise mechanism of <i>CHES1</i> as a direct transcriptional suppressor of pro-apoptotic <i>BNIP3</i> expression via its ability to recruit co-repressor complexes to the upstream regulatory region. Conversely, p53-mediated <i>CHES1</i> down-regulation is required for genotoxic stress to trigger apoptosis. Taken together, our findings provide strong support for exploiting <i>CHES1</i> as a therapeutic target in that <i>CHES1</i> antagonism would potentially lead to decreased anti-apoptotic PI3K-Akt signaling, combined reinstatement of pro-apoptotic gene expression ( <i>i.e.</i> , <i>BNIP3</i> ) and suppression of pro-survival genes, and reduced activity of oncogenic AR splice variants.					
<b>15. SUBJECT TERMS</b> Prostate cancer, forkhead, androgen receptor, p53, BNIP3, mTOR, hormonal therapy, apoptosis, chemotherapy, RNA interference, imaging					
<b>16. SECURITY CLASSIFICATION OF:</b>			<b>17. LIMITATION OF ABSTRACT</b>	<b>18. NUMBER OF PAGES</b>	<b>19a. NAME OF RESPONSIBLE PERSON</b> USAMRMC
<b>a. REPORT</b> U	<b>b. ABSTRACT</b> U	<b>c. THIS PAGE</b> U			<b>19b. TELEPHONE NUMBER</b> ( <i>include area code</i> )
			UU	30	

## Table of Contents

	<u>Page</u>
<b>Introduction.....</b>	<b>4</b>
<b>Body.....</b>	<b>4</b>
<b>Key Research Accomplishments.....</b>	<b>9</b>
<b>Reportable Outcomes.....</b>	<b>9</b>
<b>Conclusion.....</b>	<b>10</b>
<b>References.....</b>	<b>10</b>
<b>Appendices.....</b>	<b>12</b>
<b>Supporting Data.....</b>	<b>15</b>

## INTRODUCTION

Androgen is a pivotal mediator of the growth, survival, and differentiation of prostate cancer (PCa) cells. Accordingly, androgen ablation is the first-line therapy for metastatic disease and dependably mediates disease regression. Unfortunately, this treatment is only palliative, as the disease typically recurs as castration-resistant prostate cancer (CRPC) approximately two years later and accounts for the 20% mortality rate due to this neoplasm. Therefore, defining the mechanisms underlying CaP survival during androgen withdrawal (AW) and the establishment of castration resistance are critical to enhancing our understanding of disease progression and the development of more efficacious therapies. We identified *FOXP3/CHES1* (*Checkpoint suppressor 1*) as a potential molecular mediator of CaP survival during androgen ablation. Our findings demonstrated that *CHES1* exhibits an AW-induced expression pattern and is an anti-apoptotic molecule that potentially acts via induction of the phosphatidylinositol 3-kinase (PI3K)/Akt pathway and/or down-regulation of the pro-apoptotic Bcl-2 family members *BNIP3* and *BAK1*. Importantly, antagonism of its function by RNA interference (RNAi)-mediated silencing resulted in apoptotic cell death of LNCaP cells selectively in the absence of androgen. That being said, ***the operating hypothesis of this work is that CHES1 is an AW-induced gene that functions to promote prostate cancer resistance to apoptosis and can be exploited as a therapeutic target.*** Therefore, there are two general purposes of this research. The first is to achieve a better understanding of mechanisms of *CHES1* gene expression regulation and function, particularly with respect to its role in mediating apoptosis resistance during androgen ablation. Secondly, the knowledge and tools yielded from our functional studies will be utilized to test the efficacy of *CHES1*-silencing therapy (CST) in preventing the emergence of CRPC and to develop a mechanism-based non-invasive imaging strategy for monitoring the success of the therapy.

## BODY

This has been the third year of funding for this proposal and I am enthusiastically writing this report based upon the results from the work performed. Our team has been able to confirm preliminary findings described in the original grant proposal and more importantly, significantly advance these along the lines of that described in our *Specific Aims* and the *Statement of Work*. These will be described in detail below and in the *Supporting Data* section of this report. Although we did encounter technical difficulties, we have remedied these and have initiated the work that will be necessary to finish up remaining experiments in the current one-year extension.

### **Determine the position of CHES1 within the molecular hierarchy of the apoptosis regulatory network. (Tasks 11, 14)**

A major goal of this proposal is addressed by **Aim 1** to “*Define the mechanisms through which CHES1 regulates apoptosis and acts as a dominant mediator of prostate cancer survival during androgen ablation.*” One experimental approach we took to investigating this was to determine its functional position within the apoptosis regulatory network (Aim 1b), which also requires information gained from the other two sub-aims in Aim 1 as well as from Aim 2. While we originally viewed this as a “molecular hierarchy,” we now know that *CHES1* is integrated as a signaling node within a vast network and has multiple upstream regulators and functionally diverse downstream targets and effectors. I am very happy and enthusiastic to report that we have made very significant progress in this aspect of the grant and will summarize our findings in the following few paragraphs.

We have shown that androgen is a critical regulator of signal transduction and survival signaling in that AW leads to diminished AR expression, persistent hyperactivation of the PI3K-

Akt pathway, and decreased expression of the pro-apoptotic gene BNIP3. In the *2011 Annual Report*, we demonstrated that CHES1 is a dominant mediator of these events, in that enforced CHES1 expression can recapitulate the events triggered by androgen deprivation, in part through its repression of AR activity. Furthermore, we demonstrated that mTOR complex 1 (mTORC1) is a critical integration point for the survival response to decreased AR signaling and elucidated the molecular connection between AW and Akt hyperactivation (**Fig. 1A**, from 2011 Annual Report). Specifically, the results demonstrated that mTORC1 activation, as evidenced by S6K1(T389) phosphorylation, is highly dependent upon androgen (e.g., R1881) and that Akt hyperactivation results from AW-induced mTORC1 inactivation, which consequently de-represses the PI3K-Akt pathway. This was further supported by the fact that specific inhibition of mTORC1 inhibition with rapamycin results in elevated phospho-Akt (S473) levels similarly to that of AW. In the past year, we demonstrated that androgen predominantly regulates mTORC1 activation in response to amino acid (AA) signaling since AA-stimulated S6K1(T389) phosphorylation only occurred in the presence of androgen and was completely abolished during AW (**Fig. 1B**). In summary, these results demonstrate that AW- and CHES-mediated survival signaling in PCa is mediated via mTORC1 and integrates with metabolism.

Amino acid signaling to mTORC1 has been demonstrated to proceed via an interaction between mTOR-raptor (mTORC1) and Rag GTPase heterodimers and their subsequent recruitment to the surface of the lysosome (1,2). Our findings presented in the *2011 Annual Report* (**Fig. 2, A and B**) demonstrated that AW reduced the interaction of Rag heterodimers with raptor in hormone-sensitive cells (**Fig. 2A**) and that enforced expression of CHES1 was a dominant mediator of this event (**Fig. 2B**). In the current year, we provided further evidence for this mechanism by demonstrating that the requirement for androgen can be bypassed by enforced expression of a RagB mutant mimicking the GTP-bound conformation (RagB<sup>GTP</sup>) in that LNCaP cells stably expressing RagB<sup>GTP</sup> (LNCaP-FLAG-Rag<sup>GTP</sup>) exhibited androgen-independent, or insensitive, interactions between mTOR and RagB (**Fig. 2C**). Moreover, enforced RagB<sup>GTP</sup> expression overcame CHES1-mediated suppression of mTORC1 interaction with RagB/D heterodimers (**Fig. 2D**). Since mTORC1 displayed strong androgen-dependence, we hypothesized that constitutive activation of RagB<sup>GTP</sup> would confer androgen independence upon stably expressing LNCaP sublines. However, we observed that enforced activation of androgen- and amino acid-regulated mTORC1 compromises the survival of LNCaP cells in the absence of androgen in that LNCaP-RagB<sup>GTP</sup> cells exhibited a high percentage of apoptosis after extended times of culture (**Fig. 3**). While this seemed paradoxical at first, we reason that persistent amino acid signaling to mTORC1 in the absence of androgen might be interpreted as inappropriate signaling, which leads to an overall imbalance in signaling.

While our data has demonstrated that mTORC1 activation in LNCaP cells is strongly androgen-dependent, we have noted that a low level of S6K1(T389) phosphorylation always remains even upon extended periods of androgen deprivation (**Fig. 1A, lane AW-7d**). We demonstrated that this residual mTORC1 activity was derived from growth factor signaling since polypeptide growth factors such as epidermal growth factor (EGF) and transforming growth factor- $\alpha$  (TGF- $\alpha$ ) were fully capable of stimulating S6K1(T389) phosphorylation in the absence of androgen and complete absence of serum (**Fig. 4A**). These findings were reinforced in a complimentary experiment that demonstrated that low levels of S6K1(T389) phosphorylation were reinstated rapidly after removal of a PI3K inhibitor (LY294002), which completely inhibited growth factor signaling to mTORC1 (**Fig. 4B**). In contrast, full activation of TORC1 required exposure to androgen for 16-24 hours.

**Determine if repression of CHES1 expression is a critical event in p53-mediated apoptosis. (Tasks 6, 21)**

While we have demonstrated that CHES1 is a dominant mediator of anti-apoptotic signaling (e.g., PI3K-Akt hyperactivation, *BNIP3* suppression), we conversely hypothesized that its down-regulation would be necessary for an apoptotic signal to be successfully propagated in response to genotoxic agents, including mitomycin C (MMC) and adriamycin (Adr). In our *2011 Annual Report* (Fig. 5), we demonstrated that MMC-mediated apoptosis of LNCaP cells was preceded by CHES1 down-regulation and inactivation of Akt, which was consistent with the survival-promoting mechanisms described for CHES1. Since MMC and Adr are both potent inducers of p53, it was also hypothesized that CHES1 was a critical target for p53-mediated apoptosis. As reported last year, treatment of LNCaP cells with Adr (1  $\mu$ g/ml) for 4 hours markedly stimulated p53, which was accompanied by a rapid reduction in CHES1 expression (Fig. 5). Using a siRNA approach, it was further demonstrated that silencing of p53 markedly diminished both its basal expression and induction by Adr, which consequently resulted in stabilization of CHES1 levels. These experiments were completed during the current period covered by this review with the demonstration that Adr-mediated apoptosis was also diminished in the p53-silenced cells, as evidenced by the absence of PARP cleavage (Fig. 5). In conclusion, the results demonstrated that repression of CHES1 is mediated via p53 and a critical event in chemotherapy-induced apoptosis.

#### **Define the CHES1 expression profile using Affymetrix-based microarray profiling. (Task 10)**

The results discussed above enabled us to “functionally” position CHES1 within the molecular hierarchy of the apoptosis regulatory network in PCa cells. Since CHES1/FOXN3 is a member of the Forkhead box (FOX) of transcription factors, another vital goal of this grant was to further define the properties of CHES1 by characterizing its function as an anti-apoptotic transcription factor. In this regard, a major point of focus has been directed upon the pro-apoptotic gene *BNIP3* as a target of repression (*discussed below*). At the same time, we hypothesized that CHES1 has a more global influence upon PCa biology during androgen ablation through its capacity to shape the transcriptome via its action on numerous direct and indirect target genes. In order to identify the complete cohort of CHES1-regulated genes, we performed microarray-based genome-wide gene expression profiling with Affymetrix GeneChip Human Genome U133 Plus 2.0 Arrays in order to identify the genes whose expression were differentially expressed in LNCaP-*tet*-FLAG-CHES1 cells engineered for conditional overexpression of *CHES1* relative to the vector-control cell line (Fig. 6). In this experiment, *CHES1* was induced in two separate clones by treatment of the cells with doxycycline (100  $\mu$ g/ml) for 24 and 48 hours. We chose to compare doxycycline-treated FLAG-CHES1 cells to vector-only cells rather than doxycycline-treated vs. -untreated FLAG-CHES1 cells in order to 1) control for potential “leakiness” of the tetracycline-inducible system and 2) eliminate the possibility of identifying genes altered by the antibiotic alone. The results demonstrated that CHES1/FOXN3 is indeed a global regulator of transcription in that there were a total of 3,401 genes exhibiting  $\geq 1.5$ -fold change in expression (1,902 up-regulated and 1,499 down-regulated). Hierarchical clustering of the data was performed and the results depicted as heatmap (Fig. 6). Since CHES1 overexpression also mediates AR down-regulation, a significant subset of CHES1-regulated genes overlaps with genes comprising the AR transcriptome.

#### **Determine if CHES1 increases resistance to apoptosis by functioning as a transcriptional repressor of the pro-apoptotic gene BNIP3. (Task 16)**

Our previous findings have suggested that a critical, pro-survival activity of CHES1 is to function as a direct, transcriptional repressor of the pro-apoptotic gene *BNIP3* (BCL2/adenovirus

E1B 19 kd-interacting protein 3). Data supporting this notion was presented as Preliminary Findings in our proposal and in the *2011 Annual Report (Fig. 7)*. For instance, *BNIP3* reporter activity was markedly reduced during androgen withdrawal and when co-transfected with CHES1 expression constructs. Moreover, the ability of CHES1 to interact with components of transcriptional co-repressor complexes has been demonstrated previously (3). During the past year, we were able to definitively demonstrate that CHES1 is a *bona fide* transcriptional repressor of *BNIP3*.

For this, a series of experiments utilizing chromatin immunoprecipitation (ChIP) assays were performed in order to define the assembly and function of a CHES1 co-repressor complex at different regions (*labeled A-E*) across the *BNIP3* upstream regulatory region (**Fig 7A**). These were selected based upon 1) bioinformatics analysis of the *BNIP3* enhancer/promoter, which identified several loci containing forkhead-binding sites (*i.e.*, regions A, C, D) and 2) the results of ChIP-on-chip analysis (*discussed below*), which identified a CHES1-binding site approximately 1,605-bp upstream of the *BNIP3* transcription start site (**Table 1, Sequence ID# 42**). This is represented by “*region D*” and contains three forkhead binding sites within 30-bp. The initial experiment was performed in order to validate CHES1 binding to this site and to evaluate the other regions. ChIP assays performed with LNCaP cells that were either cultured in the presence or absence of DHT (1nM) for 96 hours demonstrated moderate CHES1 binding to regions A and D in the presence of androgen (2.35- and 2.75-fold enrichment, respectively), but was markedly elevated to 4.77- and 10.37-fold respectively after androgen-deprivation (**Fig. 7B**). Time-course experiments (8 to 96 hours androgen deprivation) were conducted in order to study the kinetics of CHES1 binding to region D and demonstrated that increased recruitment was evident after 24 hours, peaked at 72 hours, and persisted through 96 hours (**Fig. 7C**).

In order to determine that CHES1 was indeed participating in the assembly of a functional co-repressor complex at the *BNIP3* enhancer/promoter, we also evaluated the co-recruitment of the Sin3A co-repressor and histone deacetylase 1 (HDAC1). The functional consequences of complex formation were assessed by monitoring the levels of acetylated histone H3 (Acetyl-H3) and H4 (Acetyl-H4), as well as the presence of RNA polymerase II (RNA pol II). These experiments were performed with the tetracycline-inducible LNCaP-*tet*-FLAG-CHES1 cell line in order to have better control over CHES1 activation (*i.e.*, by adding doxycycline to the medium). The results demonstrated that the CHES1 co-repressor complex assembled at regions A and D, but much more robustly at the latter. This was evidenced by heightened enrichment of CHES1 (15.73-fold) in conjunction with Sin3A and HDAC1 (5.70- and 7.70-fold, respectively) and a concomitant reduction in the levels of acetylated histone H3 and H4 that were associated with the chromatin at that locus (**Fig. 8**). In addition, RNA polymerase II binding was reduced at the proximal promoter and transcription start site (region E). Taken together, CHES1 suppresses *BNIP3* expression via the recruitment of a co-repressor complex, which leads to epigenetic modifications in favor of a closed chromatin conformation and decreased accessibility of RNA polymerase II to initiate transcription.

In order to gain a more comprehensive understanding of how CHES1 functions as a transcriptional regulator to impact molecular and biological processes within the cell, we performed ChIP-on-chip analysis in order to identify the complete set of target genes that CHES1 binds directly to. For this, CHES1-associated chromatin DNA was precipitated in a ChIP experiment similar to that described above in **Fig. 8**, but instead of analyzing the immunoprecipitated DNA only for selected regions of interest, ChIP-on-chip analysis applies the DNA (“ChIP”) to tiling microarrays (“chip”; Affymetrix GeneChip Human Promoter 1.0R Array) in order to perform a genome-wide scan for all CHES1-binding sites represented by the CHIP DNA. Peak detection and false discovery rate (FDR) computation were performed using CisGenome software (4) and the assay revealed a novel set of 409 genome-wide recruitment

sites for CHES1; the sites having the highest enrichment are presented in **Table 1**. This information was then translated into the identification of potential CHES1 target genes by the determination of the closest genomic locus to each of these sites, as well their location relative to key functional regions (e.g., UTR, exon). As discussed above, CHES1 binding to the *BNIP3* enhancer/promoter was independently detected with this approach (Sequence ID #42, -1,605 bp to TSS). In order to determine if CHES1 target genes are biologically- and/or functionally-related, gene ontology (GO) analysis was performed (**Table 2**) using the Gene Functional Classification Tool available from DAVID (Database for Annotation, Visualization and Integrated Discovery) Bioinformatics Resources (<http://david.abcc.ncifcrf.gov/home.jsp>). This revealed the enrichment for multiple sets of genes that function in various biological processes, including negative regulation of apoptosis, nitrogen compound metabolism, and chromatin/chromosome organization. Consistent with our previous findings, GO analysis highlighted the function of CHES1 in the coordinated regulation of genes that control apoptosis. As an additional measure to identify the most significant biological processes based upon GO classifications and in an unbiased manner, we performed functional annotation clustering and this underscored that overlapping sets of CHES1 target genes are markedly enriched for those functioning in pathways that regulate apoptosis (**Fig. 9**).

While this ChIP-on-chip experiment was successful, we initially experienced delays due to tremendous difficulty in finding a commercially-available, ChIP-validated antibody that had satisfactory specificity, epitope affinity, and low background. The success of the experiment is heavily dependent on the use of a very specific antibody for immunoprecipitation of the HA or FLAG epitope-tagged CHES1 when performing the ChIP procedure with LNCaP-*tet*-HA- or FLAG-CHES1 cells. After performing the initial experiment (described in the *2011 Progress Report*), we realized that we needed a much “cleaner” antibody due to obtaining a high level of non-specific background signals. This was finally resolved by performing additional purification steps on our anti-HA and anti-FLAG antibodies (**Fig. 10**) and we are now conducting an additional experiment to validate our results.

### **Determine if implementation of *CHES1*-based therapies as adjuvants to androgen ablation will delay or prevent the emergence of castration-resistant prostate cancer (CRPC) (Tasks 12, 15, 19, 22)**

The primary goals of **Aim 3** are 1) to provide *proof-of-principle* evidence that antagonism of CHES1 function with *CHES1*-silencing therapy (CST) can prevent the emergence of castration-resistant tumors in an animal model and 2) to test a mechanism-based noninvasive imaging strategy for monitoring the success of CST. The necessary components for these experiments have been established and include LNCaP and CWR22 sublines that have tetracycline-inducible expression of *CHES1*-specific shRNA (*CHES1*-Ri) (**Task 12**) and double-stable LNCaP and CWR22 sublines infected with inducible *CHES1*-Ri expression and *BNIP3* reporter constructs, designated as LNCaP- and CWR22-*tet*-*CHES1*-Ri/*BNIP3*-*Rlu* (**Task 19**). The former were reported in the previous year's *Annual Report* and the double stable cell lines were established during the current year. However, the completion of the *in vivo* mouse studies (**Tasks 15, 22**) was substantially delayed due to obtaining very poor rates of tumor take/establishment of LNCaP-based tumors in athymic nude mice (e.g., 2 of 12 mice injected). The solution to this will be to utilize a different mouse strain, the JAX NOD-*scid*-gamma (NSG) mouse from Jackson Laboratories. Since the NSG mouse is more immunocompromised than nude mice, it is a more receptive host for xenograft tumors. We anticipate that the experiments will require a total of 6-12 months and will be completed during the *no-cost time extension*. Importantly, we validated the use of LNCaP-*tet*-*CHES1*-Ri cell lines as models for CST (**Fig. 11**). For this, LNCaP-*tet*-*CHES1*-Ri tumors were established in nude athymic mice. Bilateral orchiectomy was then

performed in order to simulate androgen deprivation and to induce endogenous CHES1 expression. CST was then started by feeding the mice doxycycline (250 mg/ml) in their drinking water to induce expression of the *CHES1*-specific shRNA. Immunoblot analysis demonstrated that CHES1 expression was markedly suppressed, which was accompanied by the consequential de-repression of pro-apoptotic BNIP3 expression and decreased levels of Akt(S473) phosphorylation.

## KEY RESEARCH ACCOMPLISHMENTS

- Demonstrated that CHES1 functions as a dominant mediator of androgen withdrawal-induced survival signaling by suppressing amino acid signaling to mTORC1, which in turn, leads to de-repression and hyperactivation of Akt.
- Demonstrated that CHES1 down-regulation is required for adriamycin-induced apoptosis and is mediated by p53-mediated transcriptional repression of CHES1 expression.
- Confirmed that *BNIP3* is a direct target of transcriptional repression by CHES1 and elucidated the mechanism to involve CHES1-mediated assembly of a co-repressor complex containing Sin3A and HDAC1 in the *BNIP3* proximal enhancer/promoter region, which consequently mediated epigenetic changes (*i.e.*, histone H3 and H4 deacetylation) that reduced accessibility to RNA polymerase II.
- Comprehensively defined the CHES1 transcriptome (gene expression profile) and cistrome (genomic recruitment sites), which provided tremendous insight into the global and dominant impact of its function upon biological processes that are critical to mediating prostate cancer progression, including the negative regulation of apoptosis.
- Validated the LNCaP-*tet*-CHES1-Ri conditionally-expressing *CHES1* shRNA cell lines as models for utilization in *proof-of-principle in vivo* studies of CHES1-silencing therapy.

## REPORTABLE OUTCOMES

### Abstracts and Presentations

1. Xiang, N., Purnell, S.M., Wee, C.B., Boucher, D.L., Shi, X.B., de Vere White, R.W., Gregg, J.P., Kung, H.J., and Tepper, C.G. Amino acid-mediated mTORC1 activation is a central integration point for androgen receptor and survival signaling in prostate cancer. Poster presented at: Keystone Symposium on "*Cancer and Metabolism*", February 12-17, 2012, Fairmont Banff Springs, Banff, Alberta, Canada.

### Development of expression vectors and cell lines

During this past year of funding, we generated several LNCaP and CWR22Pc sublines listed below:

1. Double-stable LNCaP and CWR22Pc sublines infected with inducible *CHES1* shRNA expression (CHES1-Ri) and *BNIP3* reporter constructs: LNCaP- and CWR22-*tet*-CHES1-Ri/*BNIP3-Rluc*. (**Task 19**)

### Funding applied for based on work supported by this award

1. Cancer Center Support Grant P30 (PI: de Vere White), NCI grant 2 P30 CA93373. The *CHES1/FOXN3* research supported by this grant contributed greatly to the Prostate Cancer Research Program component of the P30 renewal.
2. NIH Research Project Grant (R01) (NCI) *CHES1/FOXN3* function and regulation in cancer progression. Role: PI Proposed submission in October, 2012.

### Employment opportunities

Thankfully, the funding from this proposal continued to provide employment and training for two individuals, in addition to myself. Dr. Nong Xiang is an extremely talented and tremendously industrious postdoctoral fellow and was hired specifically for this project. She was critical in driving this project forward and was responsible for generating much of the results presented in this Annual Report. Mr. Shawn M. Purnell is another key member of the team and provided key support for maintaining cell lines, plasmid propagation, and working with Dr. Xiang and myself to complete experiments. Due to his high level of enthusiasm and initiative, he subsequently progressed to conducting experiments almost independently.

## CONCLUSION

The work in the third year of this award yielded several exciting and important findings that have contributed to both defining the fine mechanistic details of CHES1/FOXN3 action and a broader understanding of its global effects upon prostate cancer progression and persistence. Taken together, our results demonstrate that *CHES1* (*Checkpoint Suppressor 1*) is a pivotal mediator of the response to androgen ablation in that is embedded in a signaling network that responds to diminished AR signaling and engenders a strong survival response through combined actions on kinase signaling pathways and transcriptional regulation of genes. As discussed previously, our proposal was based upon preliminary findings that demonstrated that 1) that *CHES1* was an androgen withdrawal (AW)-induced gene that mediated PCa survival by potentially functioning as an anti-apoptotic transcription factor, particularly via its repression of the pro-apoptotic gene *BNIP3* and 2) that heightened *CHES1* expression was associated with key features of androgen ablation, specifically hyperactivation of the PI3K-Akt pathway and AR down-regulation. Our findings revealed that *CHES1* is a pivotal mediator of these events by acting to further suppress AR transcriptional activity, which in turn leads to mTORC1 inactivation and a consequential de-repression of PI3K-Akt signaling. Moreover, we demonstrate that while mTORC1 responds to multiple cues, androgen and *CHES1* specifically regulate its activation by amino acid signaling and at the level of the lysosome. At the same time, we fully elucidated its mechanism of action as a transcriptional regulator by demonstrating that it recruits a co-repressor complex to the *BNIP3* enhancer/promoter and has global effects in mediating survival via its direct binding to and regulation of a large cohort of genes functioning in the negative regulation of apoptosis. Consistent with this, we find that down-regulation of *CHES1* in the context of androgen ablation effectively mediates apoptosis. In addition, *CHES1* down-regulation is required for chemotherapy-induced apoptosis and is mediated by p53-mediated transcriptional repression. Taken together, our findings provide strong support for exploiting *CHES1* as a therapeutic target in that *CHES1* antagonism would potentially lead to decreased anti-apoptotic PI3K-Akt signaling, combined reinstatement of pro-apoptotic gene expression (*i.e.*, *BNIP3*) and suppression of anti-apoptotic genes, and reduced activity of oncogenic, ligand-independent AR splice variants.

## REFERENCES

1. Sancak, Y., Peterson, T.R., Shaul, Y.D., Lindquist, R.A., Thoreen, C.C., Bar-Peled, L., and Sabatini, D.M. (2008). The Rag GTPases bind raptor and mediate amino acid signaling to mTORC1. *Science* 320, 1496-1501.
2. Sancak, Y., Bar-Peled, L., Zoncu, R., Markhard, A.L., Nada, S., and Sabatini, D.M. (2010). Ragulator-Rag complex targets mTORC1 to the lysosomal surface and is necessary for its activation by amino acids. *Cell* 141, 290-303.

3. Scott, K.L., and Plon, S.E. (2003). Loss of Sin3/Rpd3 histone deacetylase restores the DNA damage response in checkpoint-deficient strains of *Saccharomyces cerevisiae*. *Mol Cell Biol* 23, 4522-4531.
4. Ji, H., Jiang, H., Ma, W., Johnson, D.S., Myers, R.M., and Wong, W.H. (2008). An integrated software system for analyzing ChIP-chip and ChIP-seq data. *Nat Biotechnol* 26, 1293-1300.

## **APPENDICES**

### 1. Abstract:

Xiang, N., Purnell, S.M., Wee, C.B., Boucher, D.L., Shi, X.B., de Vere White, R.W., Gregg, J.P., Kung, H.J., and Tepper, C.G. Amino acid-mediated mTORC1 activation is a central integration point for androgen receptor and survival signaling in prostate cancer. Poster presented at: Keystone Symposium on "Cancer and Metabolism", February 12-17, 2012, Fairmont Banff Springs, Banff, Alberta, Canada.

**Amino acid-mediated mTORC1 activation is a central integration point for androgen receptor and survival signaling in prostate cancer.**

Nong Xiang, Shawn M. Purnell, Christopher B. Wee, David L. Boucher, Xu-Bao Shi, Ralph W. deVere White, Jeffrey P. Gregg, Hsing-Jien Kung, and [Clifford G. Tepper](#). UC Davis Cancer Center and Departments of Biochemistry and Molecular Medicine, Urology, Pathology and Laboratory Medicine, UC Davis School of Medicine, Sacramento, CA 95817

The molecular mechanisms underlying prostate cancer resistance to androgen ablation are intensely studied. In the androgen-sensitive LNCaP model, diminished androgen receptor (AR) signaling represents the pivotal response to androgen withdrawal (AW) and mediates survival via hyperactivation of the PI3K-Akt pathway and elevation of Bcl-2 expression. Our results demonstrate that mTOR complex 1 (mTORC1) functions as an integrator of this response in that androgen is required to attain maximal mTORC1 activity and translation initiation complex assembly while AW markedly diminished mTORC1 activity, which consequently led to de-repression of PI3K-Akt signaling and autophagy. Concurrently, AR levels declined due to continued suppression of its translation by residual, androgen-independent, mTORC1 activity; inhibition of this remaining signal with rapamycin completely restored AR expression to levels equivalent to or exceeding that observed in the presence of androgen and recapitulated the biochemical signature of castration-resistant LNCaP-cds sublines, which are defined by elevated AR, phospho-Akt(S473), and Bcl-2 levels. In order to investigate the possibility that androgen might regulate amino acid signaling to mTORC1, we examined the interaction of mTORC1 with Rag GTPases. Notably, androgen markedly enhanced immunocomplex formation of mTOR-raptor with RagB-D heterodimers. Consistent with this finding, the androgen-dependency of this association was bypassed or attenuated by expression of RagB mutants constitutively bound to either GTP or GDP, respectively. In summary, our data demonstrate that 1) amino acid-stimulated mTOR activity represents a vital regulatory locus of androgen-mediated biology and 2) aberrant regulation of the AR-mTOR-Akt axis might represent a critical mechanism underlying the transition to castration-resistant disease.

Supported by Department of Defense PCRP Idea Award PC081032 (C.G.T.) and seed funding from the UC Davis Cancer Center.

# Amino acid-mediated mTORC1 Activation Is a Central Integration Point for Androgen Receptor and Survival Signaling in Prostate Cancer

Nong Xiang, Shawn M. Purnell, Christopher B. Wee, David L. Boucher, Xu-Bao Shi, Ralph W. deVere White, Jeffrey P. Gregg, Hsing-Jien Kung, and Clifford G. Tepper

UC Davis Cancer Center and Departments of Biochemistry and Molecular Medicine, Urology, Pathology and Laboratory Medicine, UC Davis School of Medicine, Sacramento, CA

## Abstract

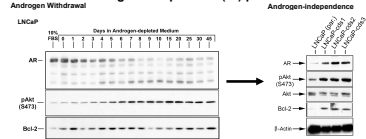
The molecular mechanisms underlying prostate cancer resistance to androgen ablation are intensely studied. In the androgen-sensitive LNCaP model, diminished androgen receptor (AR) signaling represents the pivotal response to androgen withdrawal (AW) and mediates survival via hyperactivation of the PI3K-Akt pathway and elevation of Bcl-2 expression. Our results demonstrate that mTOR complex 1 (mTORC1) functions as an integrator of this response in that androgen is required to attain maximal mTORC1 activity and translation initiation complex assembly while AW markedly diminished mTORC1 activity, which consequently led to de-repression of PI3K-Akt signaling and autophagy. Concurrently, AR levels declined due to continued suppression of its translation by residual, androgen-independent, mTORC1 activity; inhibition of this remaining signal with rapamycin completely restored AR expression to levels equivalent to or exceeding that observed in the presence of androgen and recapitulated the biochemical signature of castration-resistant LNCaP-cds sublines, which are defined by elevated AR, phospho-Akt(S473), and Bcl-2 levels. In order to investigate the possibility that androgen might regulate amino acid signaling to mTORC1, we examined the interaction of mTORC1 with Rag GTPases. Notably, androgen markedly enhanced immunocomplex formation of mTOR-raptor with RagB-D heterodimers. Consistent with this finding, the androgen-dependency of this association was bypassed or attenuated by expression of RagB mutants constitutively bound to either GTP or GDP, respectively. In summary, our data demonstrate that 1) amino acid-stimulated mTOR activity represents a vital regulatory locus of androgen-mediated biology and 2) aberrant regulation of the AR-mTOR-Akt axis might represent a critical mechanism underlying the transition to castration-resistant disease.

## Introduction

- Prostate carcinoma (CaP) is the second most common malignancy occurring in men. In 2009, approximately 235,000 new cases of CaP were diagnosed and nearly 27,000 men died from the disease.
- Androgen is a dominant mediator of CaP biology.
  - It drives growth, survival, and epithelial differentiation of both normal and malignant prostatic epithelial cells.
- Androgen ablation therapy exploits this feature to suppress androgen-AR signaling and is very effective in mediating regression.
  - However, this is only palliative and the disease typically recurs as castration-recurrent/resistant prostate cancer (CRPC), or androgen-independent (AI) CaP.
- A prominent mechanism underlying CRPC is the reinstatement of AR signaling.
  - Signified clinically by elevated serum PSA (biochemical failure).
  - AR transcriptional program is restored, albeit incompletely.
- A major reason for the failure of this therapy to cure CaP is that only a sub-population of CaP cells are killed by androgen ablation.
  - This is in marked contrast to normal prostate in which castration induces massive apoptosis of terminally-differentiated luminal cells.
- Taken together, the survival of cancerous prostatic cells is supported by both androgen-dependent and androgen-independent mechanisms.

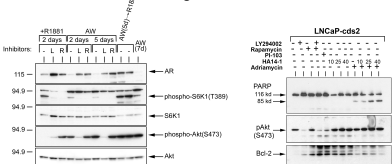
## Results

### Anti-apoptotic mechanisms are hyperactivated by androgen withdrawal and retained in androgen-independent (AI) prostate cancer cells



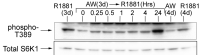
- Androgen withdrawal of androgen-dependent sensitive LNCaP cells: Diminished AR signaling hyperactivates PI3K-Akt signaling and enhances Bcl-2 expression.
- Androgen independent LNCaP-cds cell lines: Despite reinstatement of AR expression and signaling, both survival mechanisms persist and are further de-regulated.
- PI3K-Akt and Bcl-2 not only represent androgen-independent survival mechanisms, but anti-apoptotic mediators negatively regulated by AR signaling.

### mTORC1 acts as an androgen sensor and integrates the response to androgen withdrawal



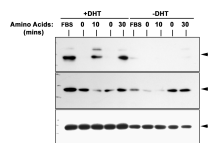
- The goal of this experiment was to investigate the regulation of mTOR by androgen signaling and its potential influence upon AR and PI3K-Akt signaling.
- Androgen was required to maintain complete activation of mTOR.
- Conversely, AW mediated a marked diminution in phospho-S6K1(T389) levels.
- However, low level, residual mTOR activity remained in the absence of androgen.
- The importance of androgen-independent (AI) mTOR activity to mediating the effects of AW is underscored by the finding that AR expression was completely restored by mTOR inhibition with LY294002 (L) or rapamycin (R).
- PI3K/Akt hyperactivation is a result of AW- or rapamycin-mediated mTORC1 inactivation.
- Although mTOR-S6K1 exhibited reversible activation by androgen, AW-induced PI3K-Akt activation was refractory to repression by subsequent androgen treatment.
- Bcl-2 expression is elevated in response to mTORC1 inhibition (right panel)

### Androgen-mediated mTOR activation proceeds with slow kinetics.



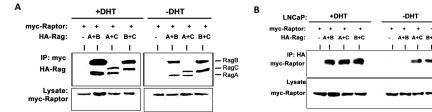
- Time-course experiments further demonstrated that while R1881 induced partial mTOR reactivation within 15 minutes, full reinstatement of phospho-S6K1(T389) levels proceeded with slow kinetics and required 24 hours.

### Androgen-AR signaling is required for amino acid-mediated mTORC1 activation.



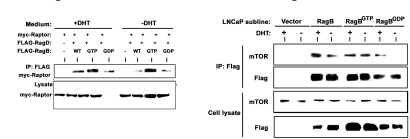
- LNCaP cells were cultured in the presence or absence of DHT for 72 hours prior to amino acid starvation 50 minutes and subsequent re-addition of amino acids for 10 or 30 minutes.
- Amino acid starvation resulted in a complete loss of mTORC1 activity, which was restored by amino acid stimulation in the presence, but not absence of androgen.

### Androgen enhances the interaction of mTORC1 with Rag GTPases



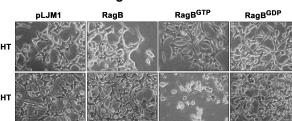
- Co-transfection and co-IP experiments demonstrated that Rag heterodimers interact with mTORC1 via raptor in an androgen-dependent manner.
- LNCaP cells were co-transfected as described above and cultured for 72 hours in the presence (+DHT) or absence (-DHT) of DHT. Co-IP analysis was performed by precipitation with anti-myc followed by immunoblotting for co-precipitated Rag complex components with anti-HA (upper panel) and control for raptor expression with anti-myc (lower panel).
- The same experiment as described in A was conducted, except co-IP analysis was performed by IP with anti-HA and subsequent analysis for Raptor (anti-myc) in the immune complex (upper panel).

### Enforced expression of a RagB<sup>GTP</sup> mutant bypasses the requirement of androgen for the interaction of mTOR with RagB/D heterodimers.



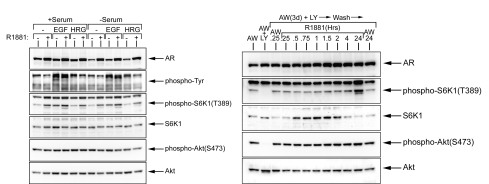
- Left panel: LNCaP cells were co-transfected with myc-raptor, RagD-WT, and different forms of RagB (WT, 54L/GTP, 99L/GDP). Cells were then cultured in the presence or absence of DHT followed by IP with anti-FLAG and immunoblot analysis for myc-raptor.
- Right panel: A similar experiment to that described above was performed using LNCaP cells stably expressing RagB, RagB<sup>GTP</sup>, or RagB<sup>GDP</sup>.

### Stable expression of RagB<sup>GTP</sup> compromises the survival of LNCaP cells in the absence of androgen.



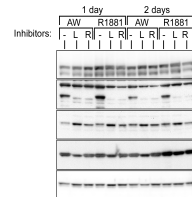
- Stable expression of RagB<sup>GTP</sup> compromises the survival of LNCaP cells in the absence of androgen.

### Polypeptide growth factors activate mTORC1 independently of androgen.



- We hypothesized that residual, AI mTOR activity was driven by serum-derived growth factors. To address this, we completely inhibited mTOR and then determined the capacity of serum and androgen to reinstate its activity.
- Basal, AI S6K1 phosphorylation was completely suppressed by PI3-K inhibition (AW+LY), but was fully restored within 15 minutes of removal of the inhibitor (AW+LY). Androgen-stimulated mTOR activity was not apparent until 4 hours after the addition of R1881 and peaked at 24 hours (AW+LY). In contrast, phospho-S6K1 levels were unchanged after the same duration in the absence of androgen (AW+LY).
- These results demonstrate that serum-derived growth factors can rapidly activate mTOR independently of androgen signaling and that androgen enhances this signal, but requires longer term signaling.

### Disruption of the AR-mTORC1-Akt signaling axis represents a critical molecular event in the transition to CRPC.



- LNCaP-cds cell lines are characterized by having greatly elevated levels of AR expression and phospho-Akt(S473) compared to the parental LNCaP.
- Like LNCaP, R1881 treatment increased T389 phosphorylation of S6K1.
- In marked contrast to LNCaP, Akt was not negatively-regulated by synthetic-androgen-induced mTOR activation:
  - Inhibition of mTORC1 with rapamycin did not induce higher levels of Akt activation.
  - Androgen-induced mTOR activation did not repress Akt, but was associated with increased Akt(S473) phosphorylation.

## Summary of Key Findings

- mTORC1 functions as a critical sensor of androgen signaling and integrates AW-induced PI3K-Akt hyperactivation, Bcl-2 up-regulation, and AR down-regulation.
- Androgen and growth factors independently activate mTOR via AR and PI3K, respectively.
- The results suggest that there is an AR-mTORC1-PI3K/Akt signaling axis. In each case, feedback-inhibitory loops are established by mTOR-mediated suppression of AR expression and PI3K activation.
- Androgen-AR signaling is required to maintain full mTORC1 activity in androgen-sensitive LNCaP cells.
- Amino acid signaling to mTORC1 is the prominent pathway influenced by androgen.
  - The ability of amino acids to activate mTORC1 is markedly diminished during androgen deprivation.
  - In contrast, serum and polypeptide growth factors can stimulate mTORC1 in both the presence and absence of androgen.
- Androgen regulates the interaction of mTORC1 with Rag heterodimers.
- The data suggest that androgen regulates the recruitment of mTORC1 to the surface of the lysosome, thereby connecting androgen deprivation with the induction of autophagy.
  - Taken together with the above findings, this is consistent with the model described for amino acid-mediated activation of mTORC1 via interaction with the Rag GTPases (Sanchez, Y et al. Science, 320:1495, 2008; Sanchez, Y et al. Cell, 141:290, 2010).
- Although enforced expression of Rag<sup>GTP</sup> can bypass the requirement for androgen to mediate mTORC1-Rag/D interactions, it does not support androgen-independent growth.
- Disruption of the AR-mTORC1-PI3K/Akt axis contributes to AW-induced AR down-regulation, Akt hyperactivation, and Bcl-2 up-regulation:
  - Growth factor driven activation of the androgen-independent mTOR component is responsible for driving down AR expression in the absence of androgen.
  - Loss of the androgen-sensitive amino acid-mTOR component results in de-repression of PI3K-Akt signaling.

## Acknowledgements

The authors are very grateful for the financial support provided by the Department of Defense PCRP Idea Award PC081032 (C.G.T.) and seed funding from the UC Davis Cancer Center. We also wish to thank the Sabatini laboratory for generously providing the mTOR, Raptor, and Rag expression constructs.

## SUPPORTING DATA

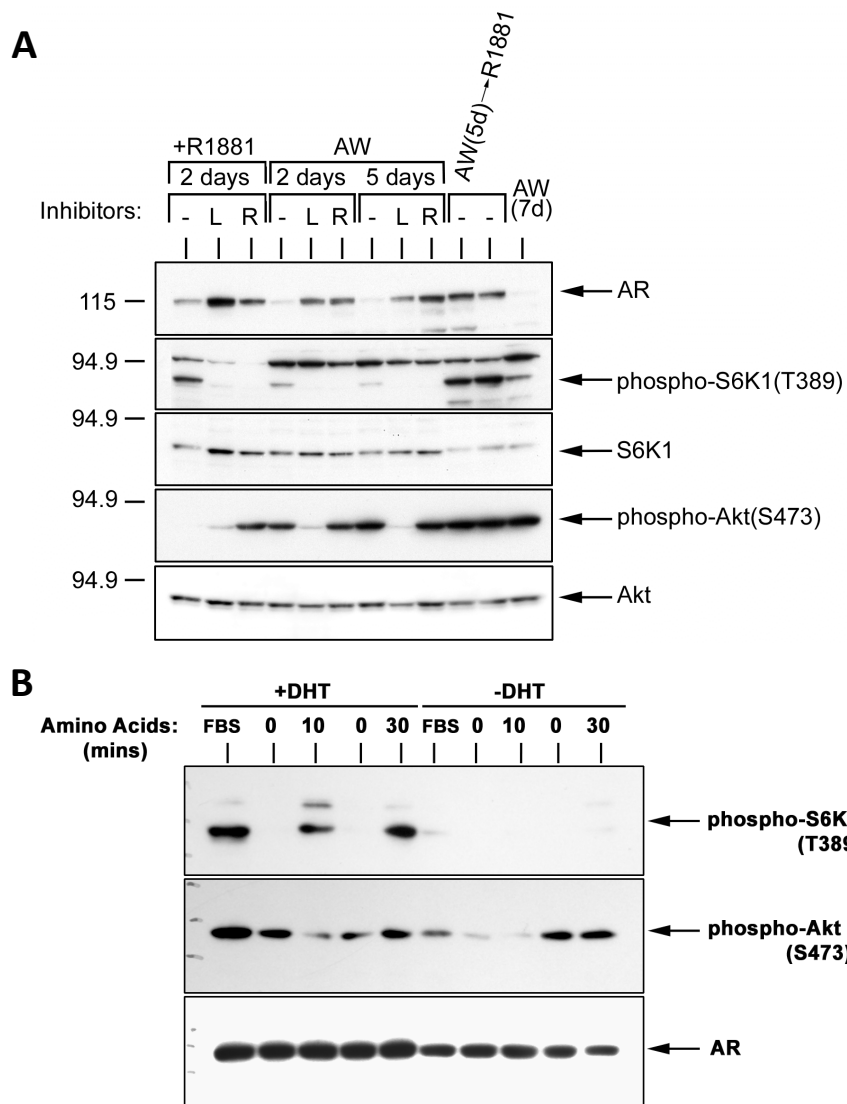


**Figure 1.** Androgen receptor signaling is a dominant regulator of mTORC1 activation by functioning at the level of amino acid signaling. **A)** Total mTORC1 activity in LNCaP cells is the sum of androgen-dependent and-independent components. LNCaP cells were treated with synthetic androgen (*R1881*; 1 nM) or subjected to AW for 2, 5, and 7 days. After 5 days of androgen deprivation, two groups of cells were also treated with *R1881* for an additional 1 and 2 days (*AW*→*R1881*). As indicated, cultures were also treated with the PI3K and mTOR inhibitors LY294002 (*L*; 10  $\mu$ M) and rapamycin (*R*; 100 nM), respectively. In addition to the determination of AR and phospho-Akt(S473) levels, mTOR activation was monitored by immunoblot analysis for Thr389 phosphorylation of S6K1. **B)** AR signaling is required for amino acid-mediated mTORC1 activation. LNCaP cells were cultured charcoal-dextran-treated FBS in the presence or absence of DHT (1 nM) for 72 hours (*FBS*) prior to amino acid starvation for 50 minutes and subsequent re-addition of amino acids for 0, 10, or 30 minutes. Immunoblot analysis was performed to evaluate levels of S6K1(T389) and Akt(S473) phosphorylation levels as well as AR expression. Amino acid starvation resulted in a complete loss of mTORC1 activity, which was restored by amino acid stimulation in the presence, but not absence of androgen.

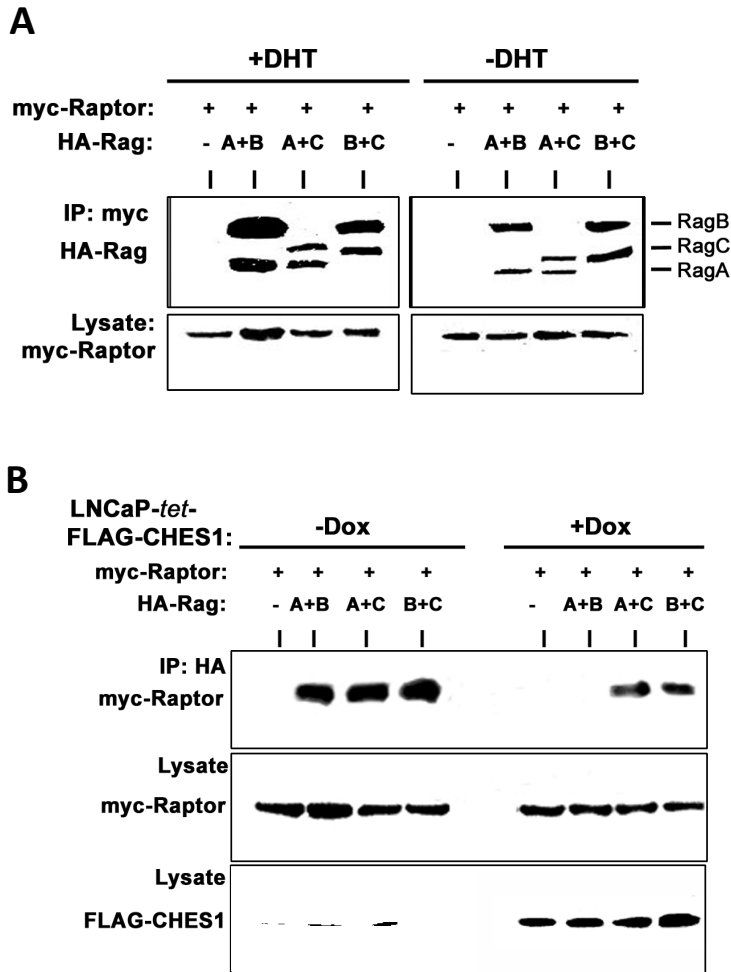


**Figure 2.** CHES1 is a dominant mediator of AW-induced mTORC1 down-regulation by suppressing Rag-raptor interactions and recruitment to the lysosome. Co-IP analysis demonstrated that Rag heterodimers interact with mTOR complex 1 (mTORC1) via raptor in an androgen-dependent manner, which is inhibited by CHES1. The regulation of this interaction was investigated by co-transfection of expression vectors for the indicated HA-tagged Rag proteins in combination with myc-tagged raptor. **A)** Androgen regulates the interaction of raptor with Rag heterodimers. LNCaP cells were co-transfected as described above and cultured for 72 hours in the presence (+DHT) or absence (-DHT) of DHT. Co-IP analysis was performed by precipitation with anti-myc (raptor) followed by immunoblotting for co-precipitated Rag complex components with anti-HA (*upper panel*) and the control for raptor expression and successful IP with anti-myc (*lower panel*). **B)** Enforced expression of CHES1 decreases Raptor-Rag interaction. LNCaP-*tet*-FLAG-CHES1 cells were transfected with myc-Raptor and HA-Rag expression vectors as described above followed by culturing in the absence (-Dox) or presence (+Dox) of doxycycline (100  $\mu$ g/ml) to induce the expression of CHES1. Co-IP analysis was performed by IP with anti-HA and subsequent analysis for Raptor (anti-myc) in the immune complex (*upper panel*). Induction of CHES1 was validated by immunoblotting with anti-FLAG (*lower panel*).

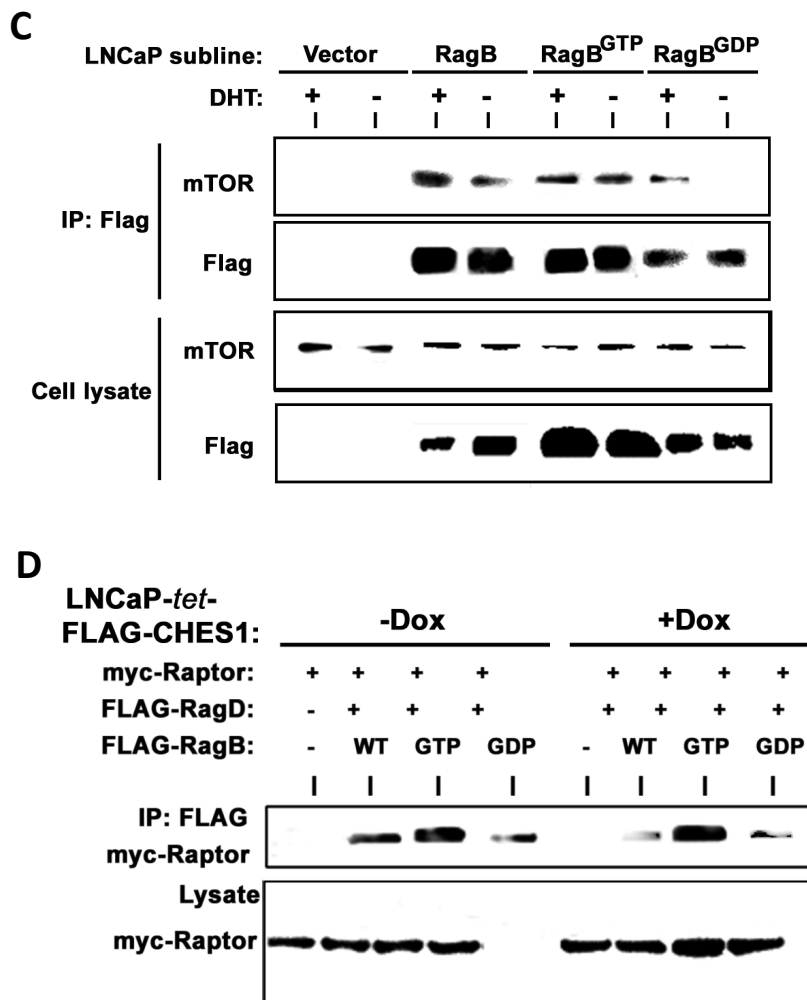


**Figure 2 (continued).** CHES1 is a dominant mediator of AW-induced mTORC1 down-regulation by suppressing Rag-raptor interactions and recruitment to the lysosome. **C)** Enforced expression of a RagB mutant mimicking the GTP-bound conformation (RagB<sup>GTP</sup>) bypasses the requirement for androgen for the interaction of mTORC1 with RagB/D heterodimers. LNCaP sublines stably expressing FLAG epitope-tagged wild-type RagB (*RagB*) and mutant forms mimicking the GTP-bound (*RagB*<sup>GTP</sup>; Q99L) and GDP-bound (*RagB*<sup>GDP</sup>; T54L) conformations were established by lentiviral infection. An empty vector control subline (*Vector*) was also generated. Cells were cultured for 3 days in the presence (+) or absence (-) of DHT (1 nM). Co-IP analysis was performed by immunoprecipitation with anti-FLAG (RagB) followed by immunoblotting for co-precipitated mTOR and RagB (*upper panel*). Cell lysates were analyzed in order to validate expression of mTOR and FLAG-RagB raptor expression. **D)** CHES1 mediates suppression of mTORC1-RagB/D interactions, which can be prevented by expression of RagB<sup>GTP</sup>. LNCaP-*tet*-FLAG-CHES1 cells were left untreated (-*Dox*) or cultured in the presence (+*Dox*) to induce overexpression of FLAG-tagged CHES1. The cells were then transiently co-transfected with expression constructs for myc-raptor, FLAG-RagD, and the indicated FLAG-RagB proteins. Co-IP analysis was performed by immunoprecipitation with anti-FLAG and subsequent immunoblot analysis for anti-myc in order to monitor levels of raptor in the FLAG-RagB/D immune complexes (*upper panel*) and in cell lysates as a control for transfection (*lower panel*).

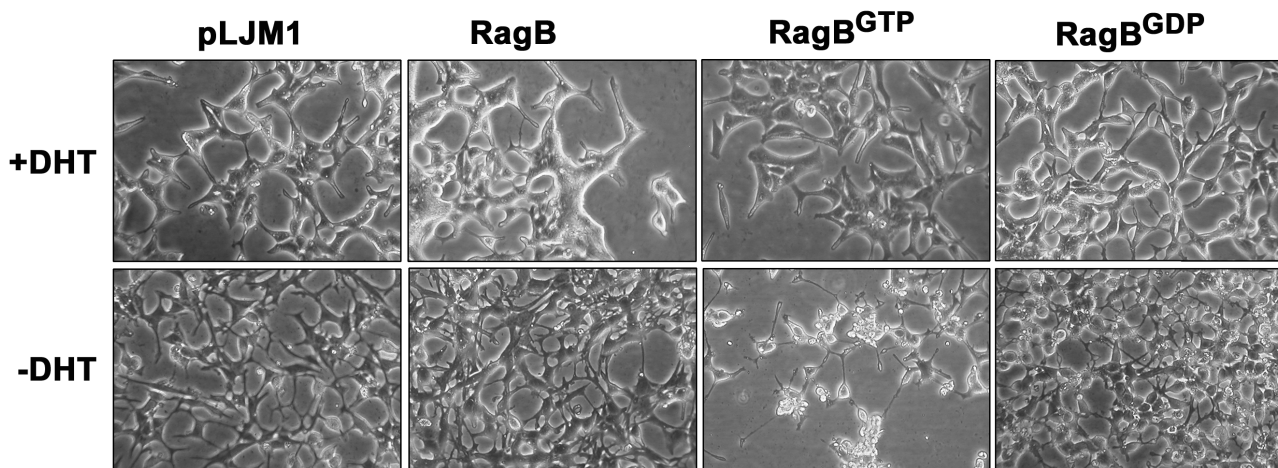


**Figure 3.** Enforced activation of androgen- and amino acid-regulated mTORC1 compromises the survival of LNCaP cells in the absence of androgen. LNCaP sublines stably expressing wild-type or mutant forms of RagB predicted to be restricted to the GTP- or GDP-bound conformations were established by lentiviral infection and subsequent selection with puromycin. As a control, an LNCaP-pLJM1 empty vector cell line was also generated. Cells were continuously cultured in both the presence (+DHT) and absence (-DHT) of androgen for 20 days and monitored by phase-contrast microscopy. As expected, LNCaP cells cultured in the absence of androgen undergo neuroendocrine differentiation as evidenced by the extension of neuritic processes. Most strikingly, and paradoxically, LNCaP-RagB<sup>GTP</sup> cells exhibited a high percentage of apoptosis when deprived of androgen (please see panel RagB<sup>GTP</sup>, -DHT).

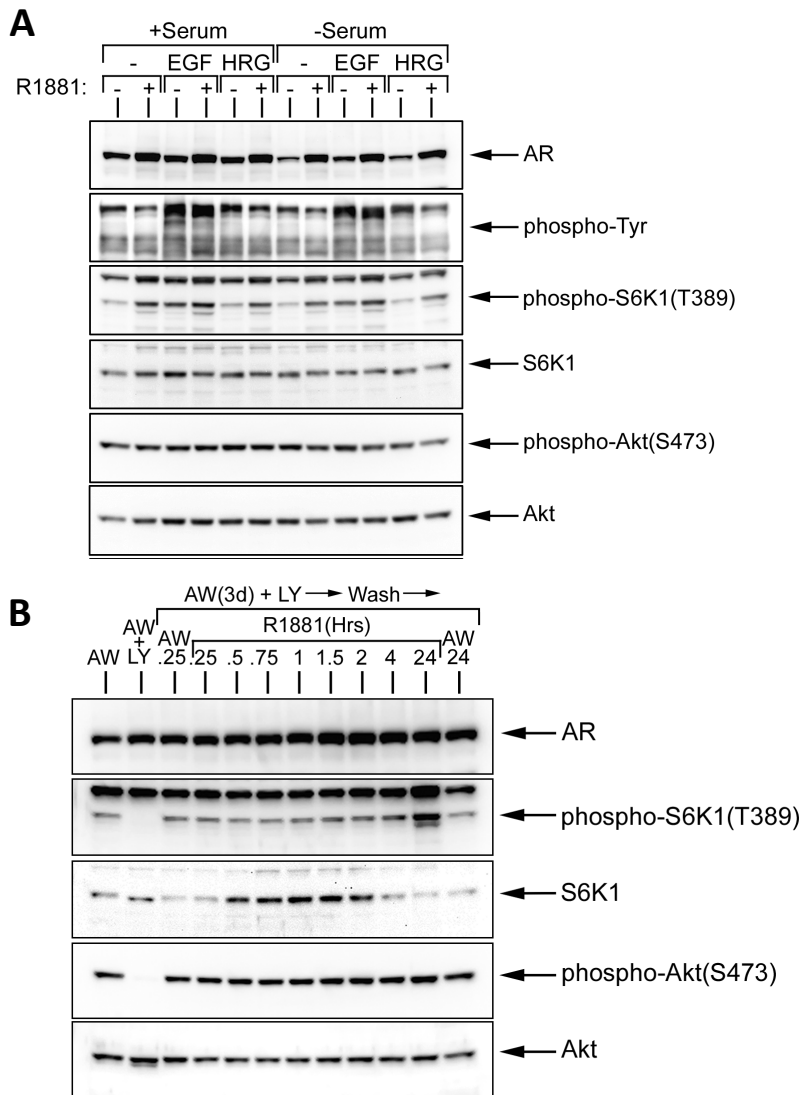


**Figure 4.** Full mTOR activation in androgen-dependent cells is mediated by both androgen and polypeptide growth factors. **A)** Androgen and polypeptide growth factors independently activate mTOR. LNCaP cells were androgen-deprived (*R1881* -) or cultured in the presence of androgen (*R1881* +; 1 nM) for 3 days. Subsequently, cultures were stimulated for 15 minutes with EGF or heregulin- $\beta$ 1 (HRG- $\beta$ 1) in the presence or absence of 10% CDT-FBS. Cell lysates were immediately prepared and immunoblot analysis performed to evaluate the phosphorylation status and expression levels of the indicated signaling molecules. In contrast to amino acid signaling to mTOR being markedly androgen-dependent, mTOR activation via growth factor-receptor tyrosine kinase signaling is fully independent of androgen. **B)** Residual, androgen-independent mTOR activity is driven by serum-derived growth factors. LNCaP cells were subjected to androgen withdrawal for 3 days (*AW*, lane 1). Complete inhibition of mTOR was achieved by treatment with LY294002 for 2 hours (*AW+LY*). Cells were then washed (*AW+LY*→*Wash*→), placed back in androgen-free medium (*AW* 0.25, *AW* 24), and then R1881 (1 nM) added in order to follow the kinetics of mTOR reactivation at the indicated times (0.25–24 hrs). Immunoblot analysis was performed to evaluate AR levels and the phosphorylation status S6K1(T389) and Akt(S473). The results demonstrate that serum-derived growth factors can rapidly activate mTOR independently of androgen signaling and that androgen enhances this signal, but requires longer term signaling (*i.e.*, hours).

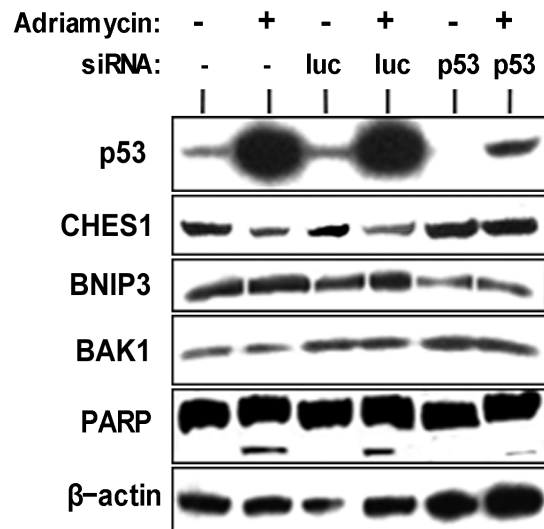


**Figure 5.** Chemotherapy-induced apoptosis requires p53-mediated repression of *CHES1* expression. The involvement of *CHES1* in p53-mediated apoptosis triggered by chemotherapeutics was investigated for adriamycin. LNCaP cells were transfected with an siRNA targeting p53 or a control siRNA directed against *Firefly* luciferase (*luc*). After 48 hours, cells were then treated with adriamycin (1 ug/ml; +) or PBS control (-) for 4 hours. Cells were harvested and immunoblot analysis performed for the expression of p53, *CHES1*, and BNIP3, Akt phosphorylation (S473), and the induction of apoptosis (PARP cleavage). Expression of  $\beta$ -actin was used as a loading control. The results demonstrate that attenuation of adriamycin-induced p53 expression leads to maintenance of *CHES1* expression and diminished apoptosis, as indicated by reduced levels of caspase-cleaved PARP.

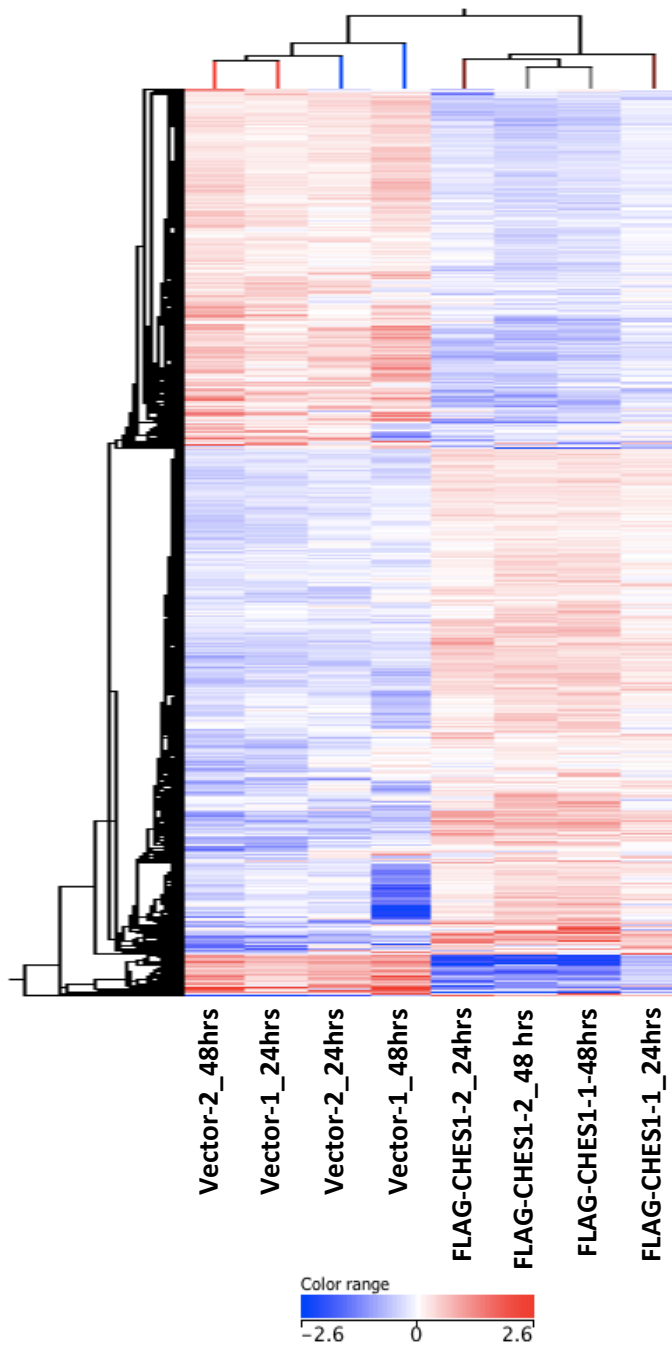


**Figure 6.** CHES1/FOXN3 is a global regulator of transcription. CHES1-regulated genes were identified using microarray gene expression profiling. Two separate clones of tetracycline/doxycycline-inducible CHES1 (LNCaP-*tet*-FLAG-CHES1) and vector-control (LNCaP-*tet*-pLVX) cell lines were treated with doxycycline for 24 or 48 hours followed by isolation of total RNA and analysis with Affymetrix GeneChip Human Genome U133 Plus 2.0 Arrays. Microarray data analysis was performed using GeneSpring GX software. Differentially-expressed genes ( $\geq 1.5$ -fold) were detected by unbiased filtering followed by hierarchical clustering in order to group genes having similar patterns of expression and to group cell lines based upon overall gene expression patterns. The results are depicted in the heat map above. Enforced CHES1 expression mediated gene expression changes in a total of 3,401 genes (1,902 up-regulated and 1,499 down-regulated).

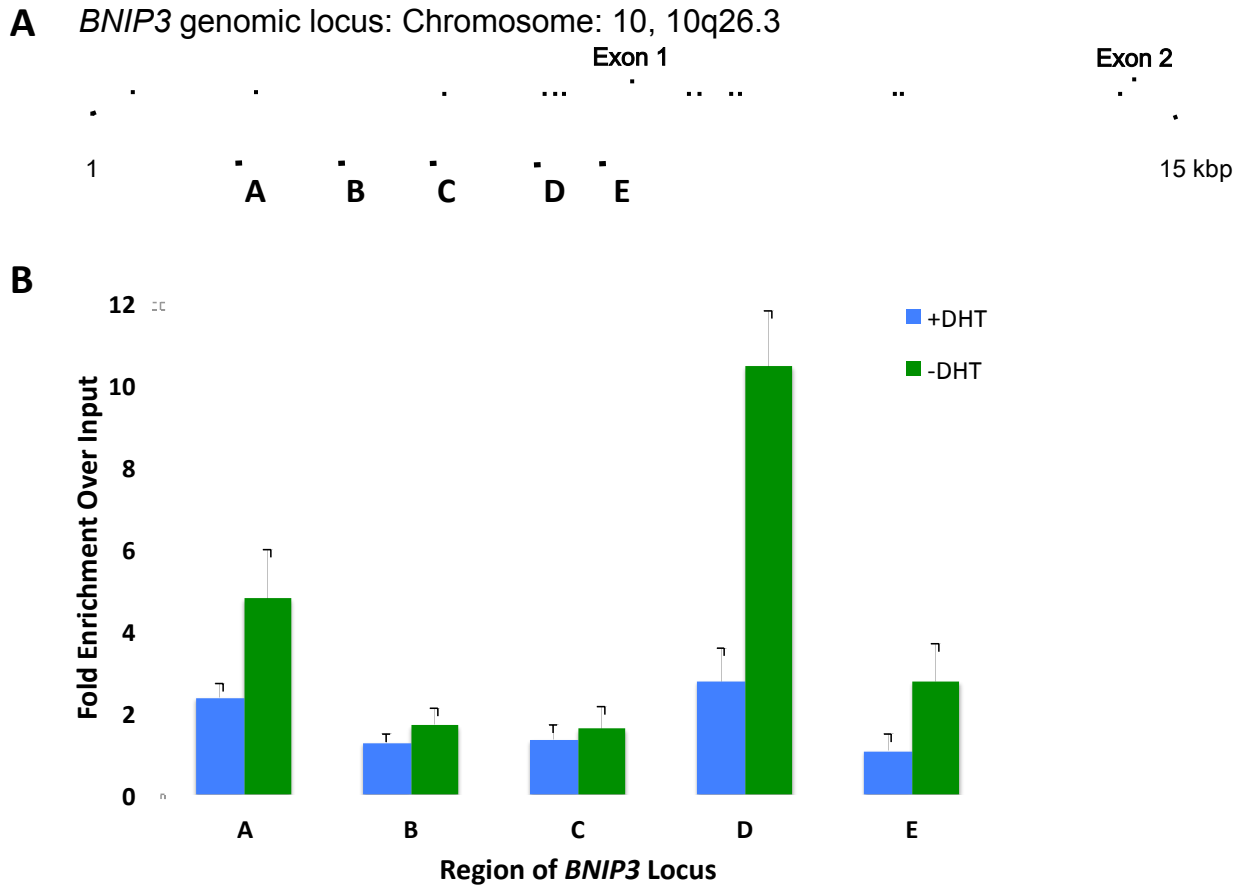


**Figure 7.** CHES1/FOXN3 is recruited to the *BNIP3* proximal enhancer/promoter in response to androgen withdrawal. **A)** Schematic of the *BNIP3* genomic locus. Screening of a 15-kbp region for forkhead/FOX consensus binding sites revealed six sites in the proximal enhancer/promoter region (tick marks). Combined with the results of the CHES1 ChIP-on-chip analysis (Table 1), 5 regions (*indicated by A-E*) were selected for the analysis of CHES1 recruitment to the *BNIP3* locus. **B)** LNCaP cells ( $4 \times 10^7$ ) were cultured in the presence (+*DHT*) or absence (-*DHT*) of DHT for 96 hours. ChIP assays were performed using rabbit polyclonal anti-CHES1 antibody (Abcam) and quantitative real-time PCR (SYBR Green) analysis of the precipitated DNA for each of the indicated regions. ChIP assays performed with non-specific IgG served as controls for non-specific binding and input DNA (*Input*) was utilized as qPCR positive control and for normalization. Results are presented as fold-enrichment in DNA bound by CHES1 relative to the input DNA level. Assays were performed in triplicate and values represent the mean  $\pm$  standard deviation. The results demonstrate that CHES1 is recruited to forkhead consensus binding sites in regions A and D and is induced by androgen withdrawal. Region D contains 3 putative binding sites and exhibited the highest level of CHES1 recruitment.

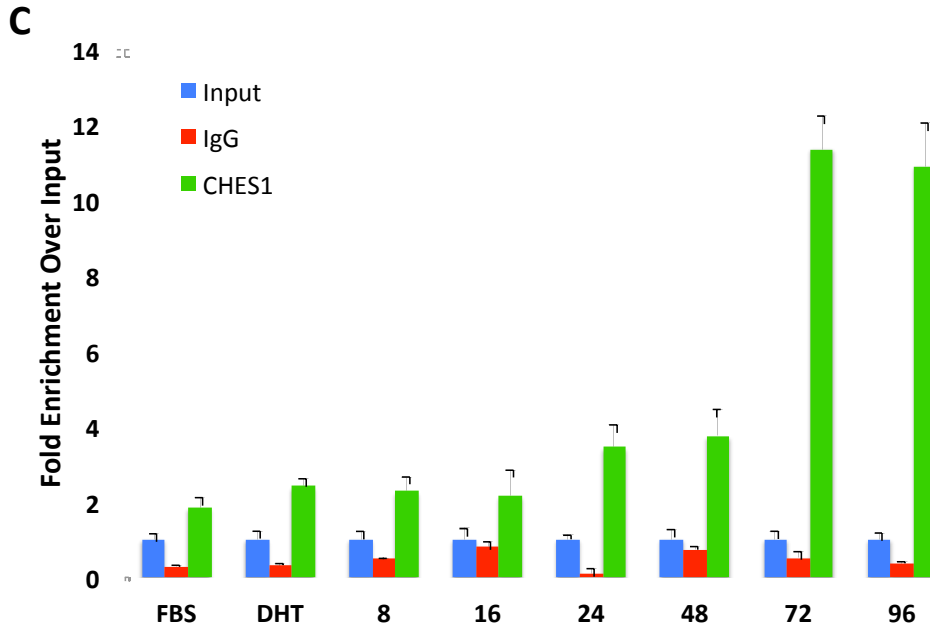


**Figure 7 (continued). C)** Kinetics of androgen withdrawal-induced CHES1 binding to the *BNIP3* regulatory region. CHIP assays were performed in a time-course analysis of CHES1 binding to *BNIP3* region D. LNCaP cells were cultured in the presence of 1 nM DHT for 96 hours (*DHT*) or subjected to androgen deprivation for 8-96 hours. Cells grown in the medium supplemented with 10% FBS (*FBS*) served as a control for complete androgen and growth factor stimulation. CHIP assays were performed as described above (Fig. 4B). Triplicate samples were analyzed for each condition. The mean fold-enrichment ( $\pm$  S.D.) in binding to region D are presented for the CHES1 and IgG (control) CHIP DNAs and for the input DNA.

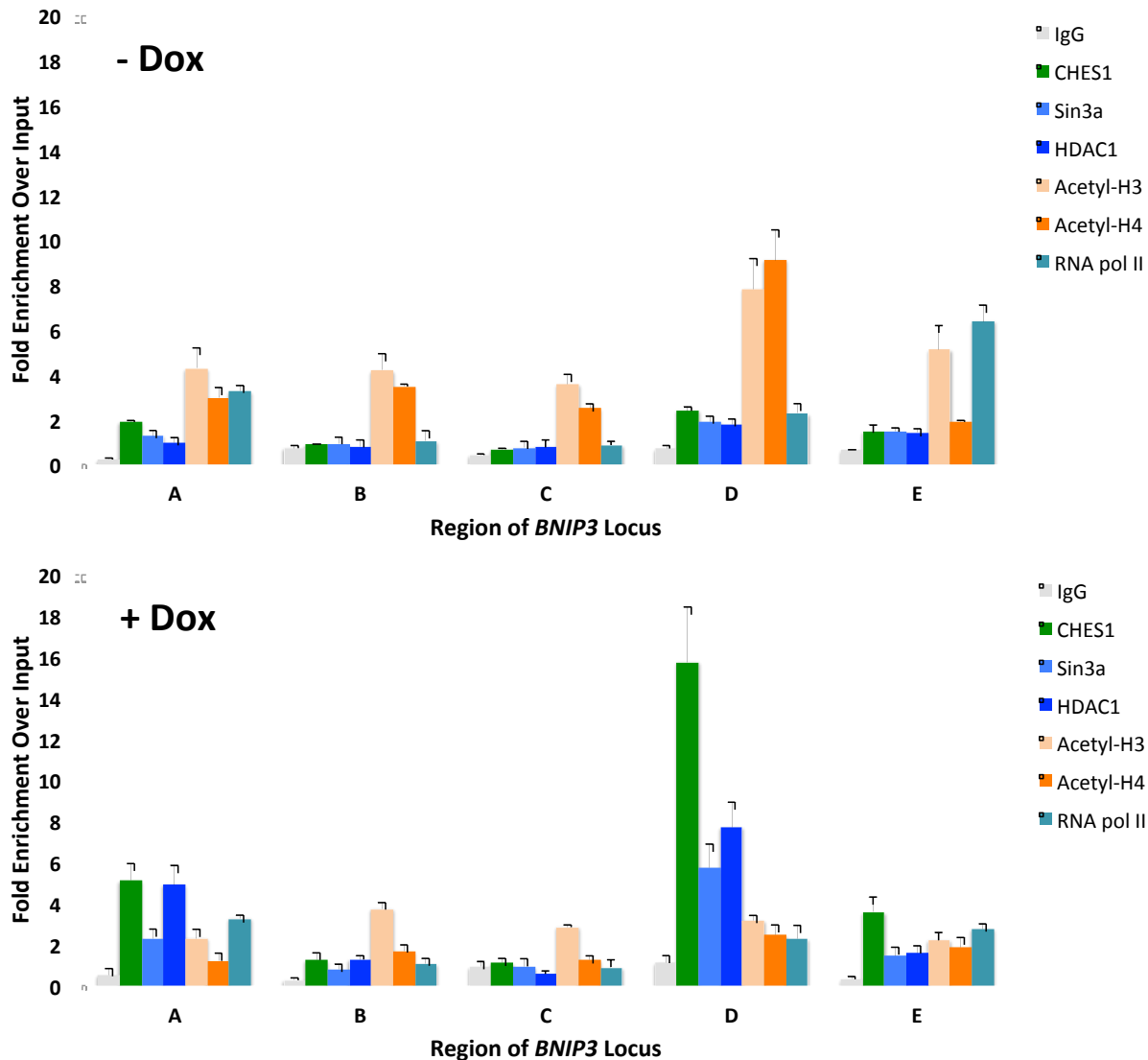


**Figure 8.** CHES1/FOXN3 participates in the assembly of co-repressor complexes at the *BNIP3* regulatory region. LNCaP-*tet*-FLAG-CHES1 cells were seeded into 10-cm dishes and allowed to reach a density of 75% confluence. The medium was then refreshed and the cells were cultured either in the absence (-*Dox*) or presence (+*Dox*) of doxycycline (100  $\mu$ g/ml). After 72 hours, the cells were cross-linked with formaldehyde and processed for ChIP assays. Soluble chromatin containing CHES1, Sin3A, HDAC1, acetylated histone H3, acetylated histone H4, and RNA polymerase II was immunoprecipitated using the corresponding antibodies specific for these proteins and epigenetic modifications. A control IgG was used to control for non-specific binding. Quantitative PCR was performed to evaluate the levels of co-regulator recruitment and chromatin modification occurring at the indicated regions of the *BNIP3* regulatory regions described in Fig. 4A. Assays were performed in triplicate and the results reported as Fold Enrichment Over Input (mean  $\pm$  S.D.) for each of the indicated chromatin immunoprecipitations and at each region (A-E).

Sequence ID	Genomic Position				Characterization of CHES1/FOXN3 Binding Sites					
	Chrom	Start	End	Strand	Size of Region Bound (bp)	Enrichment of CHES1 Binding	Closest Gene	Distance to TSS	Distance to TES	Location
1	chr11	5,707,768	5,707,963	+	196	6.4724	OR56B1	-6,457	-7,431	TSS_upstream
2	chr2	73,886,638	73,886,824	+	187	5.6014	STAMPB	-22,903	-56,786	TSS_upstream
3	chr18	14,220,299	14,220,483	+	185	5.4473	MGC26718	51,296	45,024	TES_downstream
4	chr3	157,316,623	157,316,877	+	255	5.2270	KCNAB1	-4,291	-422,336	TSS_upstream
5	chr15	43,287,147	43,287,286	-	140	5.2104	SHF	-6,552	-40,511	TSS_upstream
6	chr1	44,906,012	44,906,224	-	213	5.1395	TMEM53	6,567	-14,030	intron
7	chr7	143,565,662	143,565,794	-	133	5.0923	OR2A1	-4,860	-5,790	TSS_upstream
8	chr1	109,208,031	109,208,194	-	164	5.0666	C1orf62	-6,874	-48,058	TSS_upstream
9	chr16	65,080,679	65,080,894	-	216	4.9543	TK2	61,029	20,066	TES_downstream
10	chr14	70,063,647	70,063,822	-	176	4.8893	ADAM20	7,750	-4,903	5'UTR
11	chr19	54,184,807	54,184,946	-	140	4.8591	GSY1	3,484	-21,682	intron
12	chr15	77,179,164	77,179,466	-	303	4.8477	RASGRF1	-9,421	-137,975	TSS_upstream
13	chr6	42,829,095	42,829,305	-	211	4.8178	TBCC	-7,389	-8,963	TSS_upstream
14	chr7	106,288,413	106,288,656	+	244	4.7702	PIK3CG	-4,625	-46,286	TSS_upstream
15	chr3	126,213,254	126,213,648	-	395	4.7658	SLC12A8	200,821	70,720	TES_downstream
16	chr10	51,513,627	51,513,926	+	300	4.7572	LOC387680	16,087	-49,497	intron
17	chr1	12,756,314	12,756,601	+	288	4.7461	C1orf158	27,708	12,770	TES_downstream
18	chr3	195,663,829	195,664,044	-	216	4.6731	GP5	-62,653	-67,098	TSS_upstream
19	chr3	102,052,696	102,052,838	-	143	4.6700	ABI3BP	142,236	-101,897	intron
20	chr1	11,775,219	11,775,422	-	204	4.6587	MTHFR	13,381	-6,947	intron
21	chr7	145,442,676	145,442,951	+	276	4.6506	CNTNAP2	-1,572	-2,306,205	TSS_upstream
22	chr2	87,048,761	87,048,982	+	222	4.6319	RGPD1	-7,976	-44,498	TSS_upstream
23	chr9	21,399,502	21,399,895	+	394	4.6072	IFNA8	553	-485	exon
24	chr7	65,538,508	65,538,961	-	454	4.5819	LOC285908	-35,905	-60,256	TSS_upstream
25	chr12	87,064,088	87,064,224	+	137	4.5697	TMTC3	3,925	-51,433	5'UTR
26	chr3	152,144,805	152,145,012	-	208	4.5684	USH3A	-196	-18,268	TSS_upstream
27	chr13	19,107,114	19,107,353	+	240	4.5338	HSMPP8	1,354	-37,404	intron
28	chr1	146,426,220	146,426,696	-	477	4.5322	NBPF1	-4,416	-5,075	TSS_upstream
29	chr11	55,401,914	55,402,496	+	583	4.5273	SPRYD5	-7,826	-13,652	TSS_upstream
30	chr19	57,210,077	57,210,256	-	180	4.4939	ZNF614	13,262	-1,777	3'UTR
31	chr17	37,339,181	37,339,398	+	218	4.4900	TTC25	-1,145	-31,902	TSS_upstream
32	chr16	3,366,397	3,366,604	-	208	4.4837	ZNF434	24,525	5,586	TES_downstream
33	chr3	131,586,642	131,586,855	+	214	4.4784	FLJ35880	-46,697	-99,629	TSS_upstream
34	chrY	9,249,310	9,249,528	+	219	4.4698	TSPY2	-26,268	-29,059	TSS_upstream
35	chr6	31,351,335	31,351,629	-	295	4.4352	HLA-C	-3,649	-6,974	TSS_upstream
36	chr1	246,006,814	246,007,024	-	211	4.4352	OR1C1	-18,589	-19,531	TSS_upstream
37	chr11	7,921,377	7,921,516	-	140	4.4286	OR10A3	-3,804	-4,747	TSS_upstream
38	chr4	78,293,012	78,293,306	+	295	4.4273	CCNG2	-4,391	-13,810	TSS_upstream
39	chr2	207,257,813	207,258,082	-	270	4.4169	MDH1B	80,347	52,788	TES_downstream
40	chr8	43,268,002	43,268,160	+	159	4.4156	POTE8	1,340	-69,403	intron
41	chr1	222,102,086	222,102,358	-	273	4.3947	TP53BP2	-1,926	-68,004	TSS_upstream
42	chr10	133,797,040	133,797,475	-	436	4.3944	BNIP3	-1,605	15,836	TSS_upstream
43	chr1	12,871,396	12,871,704	-	309	4.3931	PRAMEF4	-2,939	-9,919	TSS_upstream
44	chr2	239,985,498	239,985,833	-	336	4.3858	HDAC4	1,914	-350,347	5'UTR
45	chr11	49,962,420	49,962,567	-	148	4.3800	OR4C12	-1,881	-2,809	TSS_upstream
46	chr12	6,554,032	6,554,247	-	216	4.3483	CHD4	32,672	-4,630	intron
47	chr15	46,192,995	46,193,206	+	212	4.3218	SLC24A5	-7,360	-28,779	TSS_upstream
48	chr7	138,135,644	138,135,779	-	136	4.3210	ATP6V0A4	-2,231	-94,132	TSS_upstream
49	chr3	44,724,423	44,724,603	+	181	4.2917	ZNF502	-4,628	-15,811	TSS_upstream
50	chr11	121,498,432	121,498,580	-	149	4.2905	BRCC2	-6,374	-7,235	TSS_upstream

**Table 1.** Genome-wide identification of CHES1/FOXN3 recruitment sites.

Genome-wide analysis of CHES1/FOXN3 recruitment sites was performed using ChIP-on-chip analysis with Affymetrix GeneChip Human Promoter 1.0R Array tiling arrays. FLAG-CHES1 and control IgG chromatin immunoprecipitates were prepared from doxycycline-treated LNCaP-*tet*-FLAG-CHES1 followed by DNA purification with Qiagen columns. ChIP DNA samples (anti-FLAG, control IgG) and input DNA (*i.e.*, unprecipitated, prior to IP) were then amplified and processed for microarray analysis. Data analysis was performed using CisGenome software to identify the peak intensities for all locations of CHES1 binding throughout the genome. The table lists the top 100 sites having the most enriched binding for CHES1 expressed as fold-enrichment relative to the input DNA signal (and control IgG-subtracted). Additionally, information for the exact genomic location, size of binding region. The closest gene to the binding site and its position relative to each gene's transcription start site (TSS), transcription end site (TES), 5'UTR, and exon/intron are reported. CHES1 recruitment to the *BNIP3* locus was detected as sequence/peak #42 and located 1,605 bp upstream from the TSS.

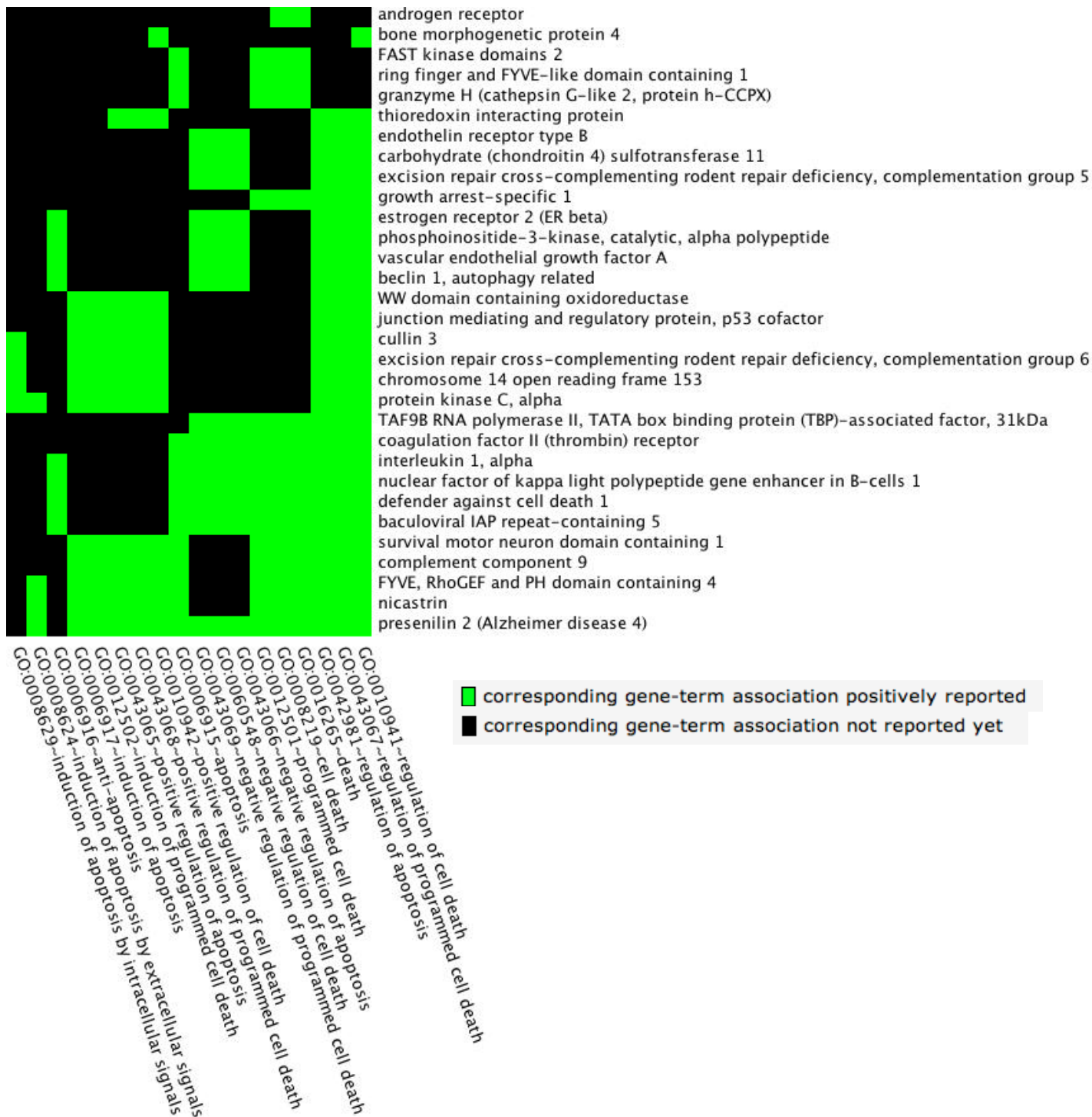
Sequence ID	Genomic Position				Characterization of CHES1/FOXN3 Binding Sites					
	Chrom	Start	End	Strand	Size of Region Bound (bp)	Enrichment of CHES1 Binding	Closest Gene	Distance to TSS	Distance to TES	Location
51	chr22	29,261,188	29,261,383	-	196	4.2558	GAL3ST1	29,590	19,338	TES_downstream
52	chr14	28,313,990	28,314,176	+	187	4.2509	FOXG1B	8,046	5,463	TES_downstream
53	chrY	9,969,614	9,969,934	+	321	4.2369	TSPY1	55,211	52,418	TES_downstream
54	chr14	19,775,012	19,775,201	+	190	4.2343	OR11H4	-5,684	-6,657	TSS_upstream
55	chr1	30,940	31,220	-	281	4.2320	FAM39B	-16,327	-26,812	TSS_upstream
56	chr5	138,112,817	138,113,016	+	200	4.2294	CTNNA1	-4,089	-185,704	TSS_upstream
57	chr7	151,565,327	151,565,474	-	148	4.2287	MLL3	1,521	-102,456	5'UTR
58	chr7	64,968,802	64,968,950	+	149	4.2124	VKORC1L1	-6,815	-88,357	TSS_upstream
59	chr1	170,654,438	170,654,623	+	186	4.2019	C1orf105	-1,922	-50,057	TSS_upstream
60	chr11	55,588,537	55,588,745	+	209	4.2011	OR8I2	-28,718	-29,649	TSS_upstream
61	chr1	32,647,686	32,647,861	-	176	4.1975	BSDC1	-15,160	-44,400	TSS_upstream
62	chr11	48,465,968	48,466,143	+	176	4.1967	OR4A47	-865	-1,792	TSS_upstream
63	chr19	58,524,602	58,524,806	-	205	4.1887	BIRC8	-38,018	-40,037	TSS_upstream
64	chr4	154,483,375	154,483,630	+	256	4.1856	MND1	-1,748	-72,190	TSS_upstream
65	chr5	64,484,532	64,484,871	-	340	4.1800	ADAMTS6	328,758	-4,382	intron
66	chr3	71,627,062	71,627,319	-	258	4.1787	FOXP1	88,639	-539,764	5'UTR
67	chr5	75,571,740	75,571,945	+	206	4.1758	SV2C	156,782	-85,329	intron
68	chr16	5,110,658	5,110,841	-	184	4.1753	FAM86A	-22,968	-35,514	TSS_upstream
69	chr9	76,294,868	76,295,033	+	166	4.1747	RORB	-7,121	-196,984	TSS_upstream
70	chr5	150,791,878	150,792,167	+	290	4.1683	SLC36A1	-15,333	-60,109	TSS_upstream
71	chr9	97,774,653	97,774,886	+	234	4.1586	C9orf102	-200	-32,205	TSS_upstream
72	chr11	106,819,914	106,820,177	-	264	4.1581	CWF19L2	10,360	-117,753	5'UTR
73	chr12	11,356,918	11,357,053	-	136	4.1546	PRB4	-2,353	-5,702	TSS_upstream
74	chr1	246,171,836	246,171,979	+	144	4.1498	OR2L13	4,792	-158,938	5'UTR
75	chr3	115,442,630	115,442,941	-	312	4.1287	ZNF80	-3,671	-6,615	TSS_upstream
76	chr1	9,918,790	9,919,028	-	239	4.1163	LZIC	6,503	-6,545	intron
77	chr17	44,374,734	44,375,037	-	304	4.1150	SNF8	2,267	-12,426	intron
78	chr19	41,824,359	41,824,530	-	172	4.1149	GIOT-1	25,134	-4,321	intron
79	chr5	27,072,006	27,072,146	-	141	4.1079	CDH9	2,369	-155,611	5'UTR
80	chr18	55,636,371	55,636,621	+	251	4.1040	PMaip1	-81,720	-86,020	TSS_upstream
81	chr11	123,121,656	123,121,916	-	261	4.1037	ZNF202	-4,214	-21,580	TSS_upstream
82	chr4	25,522,163	25,522,382	-	220	4.0970	KIAA0746	-48,731	-164,126	TSS_upstream
83	chr6	150,228,848	150,229,165	-	318	4.0952	LRP11	-1,834	-47,380	TSS_upstream
84	chr8	24,355,113	24,355,311	+	199	4.0903	ADAM7	759	-66,950	intron
85	chr17	16,550,154	16,550,372	-	219	4.0899	ZNF624	-52,381	-85,488	TSS_upstream
86	chr1	112,104,391	112,104,541	+	151	4.0883	DDX20	4,690	-7,254	intron
87	chr9	106,735,051	106,735,311	-	261	4.0744	ABCA1	-4,925	-152,075	TSS_upstream
88	chr9	68,718,863	68,719,150	-	288	4.0731	LOC441426	-48,473	-52,513	TSS_upstream
89	chr1	12,816,621	12,816,941	-	321	4.0672	HNRPCL1	14,383	13,068	TES_downstream
90	chr18	14,228,826	14,229,095	+	270	4.0671	MGC26718	59,865	53,593	TES_downstream
91	chrX	3,279,846	3,280,064	-	219	4.0574	MXRA5	-8,082	-43,348	TSS_upstream
92	chr9	3,822,601	3,822,782	-	182	4.0528	GLIS3	319,491	-8,564	intron
93	chr19	17,798,544	17,798,764	-	221	4.0509	JAK3	21,145	-694	exon
94	chr18	14,221,685	14,221,867	+	183	4.0502	MGC26718	52,681	46,409	TES_downstream
95	chr20	38,758,390	38,758,572	-	183	4.0436	MAFB	-7,192	-10,549	TSS_upstream
96	chr7	94,299,170	94,299,353	+	184	4.0428	PPP1R9A	-75,623	-464,399	TSS_upstream
97	chrY	25,412,187	25,412,366	+	180	4.0409	DAZ3	-43,372	-93,666	TSS_upstream
98	chr15	80,558,472	80,558,926	-	455	4.0401	RPS17	53,220	49,516	TES_downstream
99	chr11	5,499,342	5,499,653	-	312	4.0372	UBQLNL	-11,769	-14,390	TSS_upstream
100	chr19	57,314,518	57,314,746	-	229	4.0349	ZNF616	20,370	-5,167	intron

Table 1 (continued). Genome-wide identification of CHES1/FOXN3 recruitment sites.

GO Term Annotation Number	GO Term	Count	%	Fold Enrichment	P Value
GO:0065003	macromolecular complex assembly	31	7.3113	1.9168	7.92E-04
GO:0043933	macromolecular complex subunit organization	31	7.3113	1.7953	0.00218785
GO:0010604	positive regulation of macromolecule metabolic process	31	7.3113	1.4874	0.02746072
GO:0009057	macromolecule catabolic process	29	6.8396	1.5268	0.024877796
GO:0010941	regulation of cell death	27	6.3679	1.3622	0.092303397
GO:0031328	positive regulation of cellular biosynthetic process	25	5.8962	1.5007	0.045247178
GO:0009891	positive regulation of biosynthetic process	25	5.8962	1.4791	0.051381209
GO:0044265	cellular macromolecule catabolic process	25	5.8962	1.4179	0.078646781
GO:0051173	positive regulation of nitrogen compound metabolic process	24	5.6604	1.5324	0.041376265
GO:0034622	cellular macromolecular complex assembly	23	5.4245	2.9740	1.03E-05
GO:0034621	cellular macromolecular complex subunit organization	23	5.4245	2.6491	5.99E-05
GO:0010557	positive regulation of macromolecule biosynthetic process	23	5.4245	1.4461	0.076061649
GO:0006325	chromatin organization	22	5.1887	2.3931	3.70E-04
GO:0051276	chromosome organization	22	5.1887	1.8652	0.007523387
GO:0045935	positive regulation of nucleobase, nucleoside, nucleotide and nucleic acid metabolic process	22	5.1887	1.4497	0.080934474
GO:0051603	proteolysis involved in cellular protein catabolic process	21	4.9528	1.4391	0.094614443
GO:0044257	cellular protein catabolic process	21	4.9528	1.4320	0.096643363
GO:0045941	positive regulation of transcription	20	4.7170	1.4581	0.093117178
GO:0051254	positive regulation of RNA metabolic process	19	4.4811	1.6242	0.045643313
GO:0045893	positive regulation of transcription, DNA-dependent	18	4.2453	1.5516	0.07306722
GO:0043066	negative regulation of apoptosis	14	3.3019	1.6262	0.090762589
GO:0043069	negative regulation of programmed cell death	14	3.3019	1.6035	0.0976572
GO:0006333	chromatin assembly or disassembly	14	3.3019	4.5328	1.25E-05
GO:0051094	positive regulation of developmental process	12	2.8302	1.7749	0.07656331
GO:0006334	nucleosome assembly	11	2.5943	5.3846	3.45E-05
GO:0031497	chromatin assembly	11	2.5943	5.1989	4.68E-05
GO:0065004	protein-DNA complex assembly	11	2.5943	4.9704	6.91E-05
GO:0034728	nucleosome organization	11	2.5943	4.8635	8.32E-05
GO:0006323	DNA packaging	11	2.5943	3.8658	5.51E-04
GO:0040007	growth	11	2.5943	2.4716	0.013862896
GO:0007398	ectoderm development	10	2.3585	2.0663	0.053414179
GO:0009100	glycoprotein metabolic process	10	2.3585	2.0356	0.057963787
GO:0032583	regulation of gene-specific transcription	9	2.1226	2.7617	0.01637838

**Table 2.** Biological processes regulated by CHES1.

Gene ontology (GO) analysis was performed on the genes located in close proximity to the newly-identified CHES1 binding sites listed in Table 1. This was accomplished using the Gene Functional Classification Tool available from DAVID (Database for Annotation, Visualization and Integrated Discovery) Bioinformatics Resources (<http://david.abcc.ncifcrf.gov/home.jsp>) in conjunction with the GO Biological Pathways database. The biologically- and functionally-related groups of genes are listed by their respective GO Terms and ranked on the basis of the number of CHES1-bound genes (*Count*) associated with each group. The over-representation and statistical significance of each functional group is represented by *Fold Enrichment* and *P Value*, respectively. The function of CHES1/FOXN3 in regulating promoting survival is underscored by its potential regulation of at least 27 genes that function apoptosis-associated pathways including the *regulation of cell death*, *negative regulation of apoptosis*, and *negative regulation of programmed cell death*.



**Figure 9.** Apoptosis-associated genes are key binding targets of CHES1. Gene Ontology analysis was performed on the 409 target genes identified by CHIP-on-chip analysis of CHES1/ FOXN3 binding sites in LNCaP cells (Tables 1 and 2). In order to further identify the most over-represented functional groups of genes and consolidate the information, we also applied the DAVID Functional Annotation Clustering Tool (<http://david.abcc.ncifcrf.gov/home.jsp>). This revealed that CHES1 target genes are markedly enriched for those functioning in pathways that regulate apoptosis.

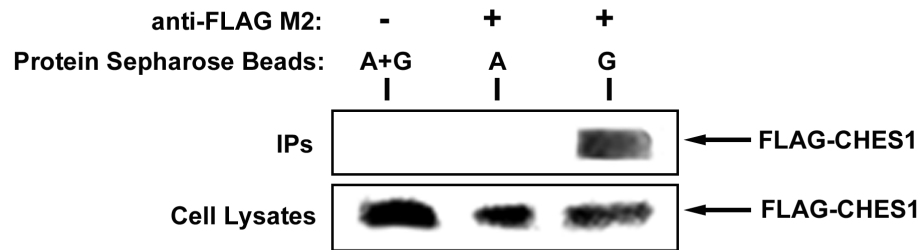


**Figure 10.** Optimization of conditions for immunoprecipitation (IP) of FLAG-tagged CHES1. LNCaP-*tet*-FLAG-CHES1 cells were cultured in medium supplemented with doxycycline (100  $\mu\text{g}/\text{ml}$ ) for 3 days. Cells were lysed in standard NP-40 lysis buffer and cytosolic extracts prepared. FLAG-CHES1 was immunoprecipitated from aliquots of 1 mg total protein with anti-FLAG M2 monoclonal antibody (5  $\mu\text{g}$ ) and captured with Protein A- or G-Sepharose (*lanes 2 and 3*). As a control for non-specific protein binding to the Sepharose beads, an incubation was performed in which primary antibody was not added (*lane 1*). Eluted immunocomplexes and corresponding cytosolic extracts were then analyzed by immunoblot analysis with anti-FLAG antibody. As shown, FLAG-CHES1 was efficiently and specifically immunoprecipitated using anti-FLAG M2 antibody in combination with Protein G-Sepharose.

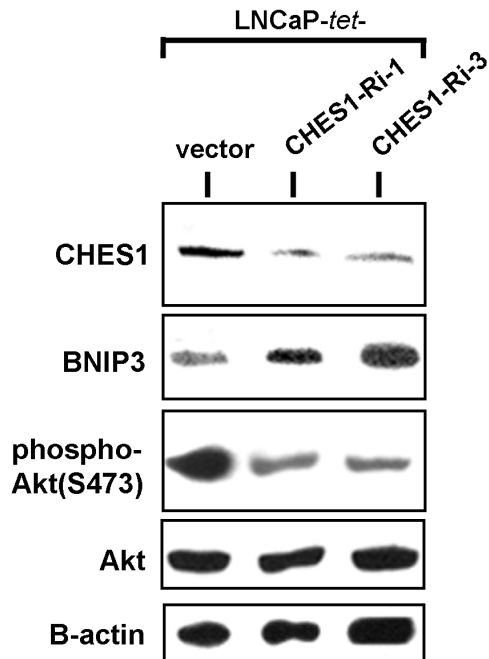


**Figure 11.** Validation of the LNCaP-*tet*-CHES1-Ri cell lines as models for use in *CHES1*-silencing therapy (CST). LNCaP-*tet*-CHES1-Ri tumors conditionally expressing *CHES1* specific shRNAs were established in nude athymic mice by subcutaneous injection of  $1 \times 10^7$  cells into nude athymic mice previously implanted with time-release testosterone pellets. When the tumors reached a diameter of 0.3 cm, bilateral orchiectomy was performed in order to simulate androgen deprivation and to induce endogenous *CHES1* expression. After fourteen days post-castration, CST was commenced by feeding the mice doxycycline (250  $\mu\text{g}/\text{ml}$ ) in their drinking water to induce expression of the *CHES1*-specific shRNA. Tumors were harvested 7 days later and flash-frozen in liquid nitrogen. Immunoblot analysis was performed to evaluate the levels of the indicated proteins and/or phosphorylation status. The results demonstrated that shRNA-mediated silencing of *CHES1* expression can potentially enhance apoptosis *in vivo* through the combined down-regulation of anti-apoptotic Akt signaling and de-repression of pro-apoptotic BNIP3 expression.